Evaluation of the Salinic I tectonic, Cancañiri glacial and Ireviken biotic events: Biochemostratigraphy of the Lower Silurian succession in the Niagara Gorge area, Canada and U.S.A.

Uwe Brand [a,*], Karem Azmy [b], Jan Veizer [c]

[a] Department of Earth Sciences, Brock University, St. Catharines, Ontario, Canada L2S 3A1
[b] Department of Earth Sciences, Memorial University of Newfoundland, St. John's, Newfoundland, Canada A1B 3X5
[c] Ottawa-Carleton Geoscience Centre, University of Ottawa, Ottawa, Ontario, Canada K1N 6N5

Received 17 August 2004; received in revised form 6 May 2005; accepted 7 March 2006

Abstract

Well-preserved brachiopods from the Niagara Gorge area, Anticosti Island, Britain, Gotland and Estonia were utilised to delineate a complex isotopic evolution for Llandovery–Wenlock seawater. The Sr-isotope record reflects the Salinic I tectophase of the Late Llandovery in the continuous increase in $^{87}Sr/^{86}Sr$ values from 0.708070 to 0.708346. The Salinic II tectophase is marked by relative constancy of Sr isotope values until the Late Wenlock when it rises from 0.708345 to 0.708430. The second tectonic phase was therefore likely only of a regional nature. The carbon isotopes during the Llandovery fall within a band of about −1‰ to +3‰, a range comparable to modern low-latitude brachiopods. A large positive $\delta^{13}C$ excursion of about 3‰, identifies the Ireviken event/excursion, characterizes the Early Wenlock. The biotic crisis and the isotope excursion itself may be ultimately related to the onset and duration of the Cancañiri glaciation, although a direct causative scenario is as yet unknown. The oxygen isotopic trends of well-preserved brachiopods clearly reflect a warm climate interval during the latest Llandovery associated with the Silurian sea level highstand. Subsequently, in the Early Wenlock, the sea level fell with the onset of the Cancañiri glaciation in the southern hemisphere. This is reflected in a significant positive $\delta^{18}O$ excursion, particularly in brachiopods from the Niagara Gorge area. Brachiopods from lower latitudes were awash in warm tropical currents and therefore exhibit somewhat more negative $\delta^{18}O$ values, indicating a lesser cooling gradient.

Keywords: Llandovery–Wenlock; Appalachian Basin, Niagara Gorge; Carbon, oxygen strontium isotopes; Salinic I tectonic event; Ireviken biotic event/excursion; Cancañiri glacial event

1. Introduction

Biochemostratigraphic research is making great strides in identifying and defining geological events, in particular those related to glacial and biotic phenomena (e.g., Brenchley et al., 1994; Marshall et al., 1997; Veizer et al., 1997, 1999; Azmy et al., 1998; Ruppel et al., 1998; Mii et al., 1999; Brand et al., 2004). Unfortunately, detailed stratigraphic information and biogeochemical data are still rare for many of these events, hindering elucidation of cause and effect relationships and resolution of the progression of temporal events. For the Early Silurian, however, recent detailed isotope studies, based on brachiopods, conodonts and carbonate matrices from Gotland,

* Corresponding author. Tel.: +1 905 688 5550x3529; fax: +1 905 682 9020.
E-mail address: uwe.brand@brocku.ca (U. Brand).

0031-0182/$ - see front matter © 2006 Elsevier B.V. All rights reserved.
doi:10.1016/j.palaeo.2006.03.004

Estonia, England, North America and Australia (e.g., Talent et al., 1993; Samtleben et al., 1996; Wenzel and Joachimski, 1996; Azmy et al., 1999; Fig. 1), enable us to utilize this database in an attempt to elucidate the geological meaning of the Early Silurian isotope record of the Niagara Gorge.

The Appalachian Foreland Basin, including the sediments of the Niagara Gorge, was created in part by the collision of Laurentia with arc terrains during the Taconic Orogeny (Brett et al., 1998). The basin received, on an intermittent basis, siliciclastic sediments shed from the highlands, and occasionally carbonates deposited in a subtropical setting at about 23–30°S paleolatitude (Fig. 1). Tropical storms and hurricanes are believed to have exerted a significant impact on the depositional milieu of the Appalachian Foreland Basin (Brett et al., 1998). Subsequent to the Taconic event, a 'new' pulse of tectonic activity, recently named the Salinic Orogeny, affected the eastern margin of Laurentia (Ettensohn and Brett, 1998), but the impact and importance of this tectonic event, regional or global, is as yet unresolved. The sequence of the Appalachian Foreland Basin is divisible into sedimentary cycles of varying scales (Brett et al., 1998), some of them related to sea level high- or lowstands, with variable influx of sediments on thousand to million year time scales (e.g., Brett et al., 1990; Kidwell and Bosence, 1991; Meyers and Milton, 1996).

Other events that may have had an impact on the configuration of the Appalachian Foreland Basin and the nature of its sedimentary fill include Early Silurian glacial episodes recognized in South America (Hambry, 1985; Grahn and Caputo, 1992; Caputo, 1998). Outcrops of glaciomarine tillites are widespread throughout South America and are considered to belong to the Cancañiri Formation (Hambry, 1985). According to Hambry (1985, p. 281) "... age of the formation is restricted to the Ashgill–Wenlock interval, and palynological evidence suggests that it is almost entirely of Wenlock age." Subsequent biostratigraphic work, using graptolites and chitonozoans (Grahn and Paris, 1992) on the tillites in Brazilian basins recognized four glacial episodes, with the youngest also being the most widespread one (Grahn and Caputo, 1992). Based on the shelly fauna this youngest and fourth tillite is "... dated as Late Telychian to earliest Wenlock ..." (Grahn and Caputo, 1992, p. 14). This widespread and extensive fourth glacial episode during the latest Telychian–earliest Wenlock in Gondwana, potentially of global significance, may have coincided, in part, with the Ireviken biotic event. This biotic event was recognized from the Lower Silurian faunal changes on the island of Gotland, Sweden

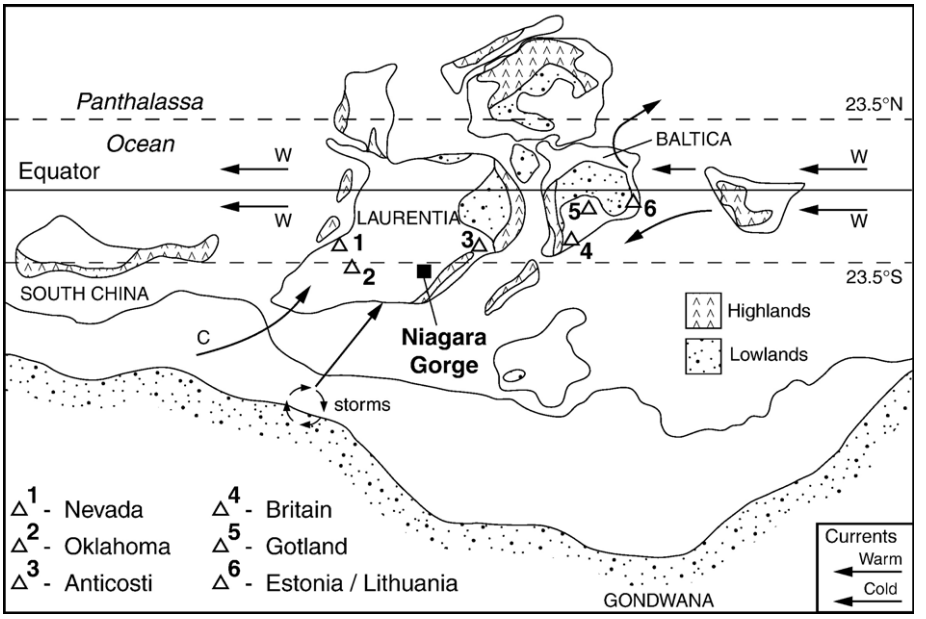

Fig. 1. Early Silurian paleogeography and location of the study area in Ontario/New York State. The Appalachian Foreland Basin is located from about 23°S in New York State to about 30°S of Laurentia (Wilde, 1991). The Niagara Gorge area is located between Ontario and New York State and locations of other studies are: 1) Nevada (Saltzman, 2001), 2) Oklahoma (Ruppel et al., 1996, 1998; Saltzman, 2001), 3) Anticosti Island (Wadleigh and Veizer, 1992; Ruppel et al., 1996, 1998; Azmy et al., 1998, 1999), 4) Britain (Azmy et al., 1998, 1999), 5) Gotland, Sweden (Wadleigh and Veizer, 1992; Wenzel and Joachimski, 1996; Azmy et al., 1998, 1999; Samtleben et al., 2001; Munnecke et al., 2003), and 6) Estonia/Lithuania (Azmy et al., 1998, 1999; Heath et al., 1998). Arrows are the hypothetical track of currents, c — cold, w— warm (modified from Driese et al., 1991; Wilde et al., 1991; Brett et al., 1998).

(Walliser, 1964; Jeppsson, 1987, 1998; Munnecke et al., 2003) and is claimed to have been the major biotic crisis of the Silurian Period (Talent et al., 1993). Support for such a view comes from a host of widely distributed locations in Australia, Britain, the Urals, Poland, Estonia and North America (Jeppsson, 1998).

The Niagara Gorge area is another supporting locality with its complementary high-resolution Early Silurian isotope records. In the present study, brachiopods were collected from rocks of the Neagha, Reynales, Merritton, Irondequoit and Rochester Formations of the Clinton Group that are exposed along the Niagara Escarpment in southern Ontario and western New York State (Figs. 2 and 3) and described in detail by several authors (e.g., Brett et al., 1990, 1995, 1998; Loduca and Brett, 1994; Brett and Goodman, 1996). The stratigraphy (Fig. 3), in an ascending order, is: 1) the Neagha Formation a grey-green shale and an underlying unnamed pink-grey arenaceous carbonate unit, both replete with fossils; 2) the Reynales Formation consisting of dolomicrite, biosparite, shale and phosphatic limestone replete with invertebrate fossils; 3) the Merritton Formation, a pink-grey limestone with intercalated arenaceous carbonate layers and abundant Pentameroides sp. in the upper part of the formation; 4) the Irondequoit Formation, subdivided into the Rockway and Model City Members and consisting of 2–3 m crinoidal, variably dolomitized packstones and grainstones with small bryozoan–algal mounds; and 5) the Rochester Formation that varies in thickness from 1 m in the Hamilton area (Ontario) to over 40 m east of Rochester (New York State) and consists of grey shale/mudstone. The formation contains highly fossiliferous limestone beds throughout, and is subdivided into the Lower Lewiston and the Upper Burleigh Hill Members.

Our study of the Early Silurian beds in the Niagara Gorge area has three major objectives: 1) development of a high-resolution biochemostratigraphic records (C, O, Sr isotopes) for the Early Silurian using unaltered brachiopods, 2) documentation of geochemical trends in the context of coeval tectonic, glacial and biotic events. Specifically, we hope to compare inversions in the geochemical trends to the onset and duration of tectonic, biotic and glacial events during the Llandovery–Wenlock transition, and 3) correlation of the biochemostratigraphy of the Niagara Gorge area and the Anticosti/Gotland sections (Azmy et al., 1998, 1999) with similar Early Silurian records elsewhere.

2. Methods

A total of 142 samples (126 brachiopods, 15 matrices, 1 cement) were analyzed for trace elements, stable and radiogenic isotopes (Appendix). Brachiopods were extracted from the surrounding rock, cleaned by physical and chemical means (e.g., leached with 10% HCl until specimens were deemed clean), rinsed with distilled water, and left to air-dry. For surrounding rocks (matrix), all extraneous biogenic fragments and weathered material were removed. Brachiopods, mostly as fragments, were examined visually and by scanning electron microscope for physical preservation of microstructural layers and of their individual fibers. Up to 100 mg of powder was digested in 5% (v/v) HCl for 70–80 min. After filtration, the non-carbonate portion (IR — insoluble residue) was determined gravimetrically by ashing the filtrate. All glass and plastic ware was cleaned with aqua regia. N.B.S. (now NIST) and U.S.G.S. SRMs (standard reference materials), 634, 636, 19-IAEA, 987, EN-1, sample duplicates and blanks, were analyzed to satisfy QA/QC requirements (Brand and Veizer, 1980). The IR, Ca, Mg, Sr, Fe and Mn were determined for most samples (Appendix), with elemental analyses carried out on a

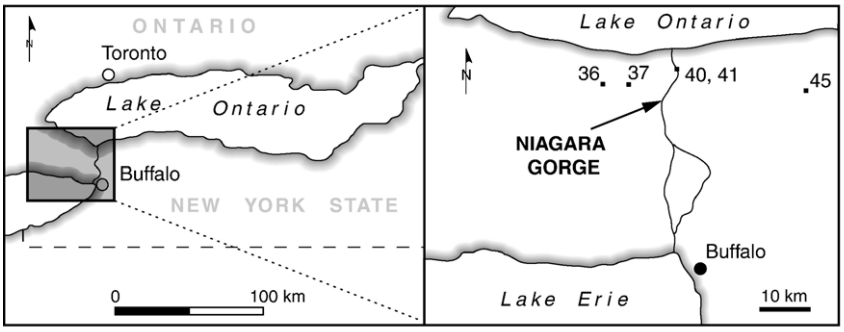

Fig. 2. Locality map of Silurian sampling sites in the Niagara Gorge area of southern Ontario and western New York State (36: Burleigh Hill, St. Catharines, Ontario; 37: Lock #5, Thorold, Ontario; 40 and 41: Niagara Falls Gorge, Artpark, New York State; 45: Hydro Road, Rochester, New York State). For general location within Laurentia see Fig. 1.

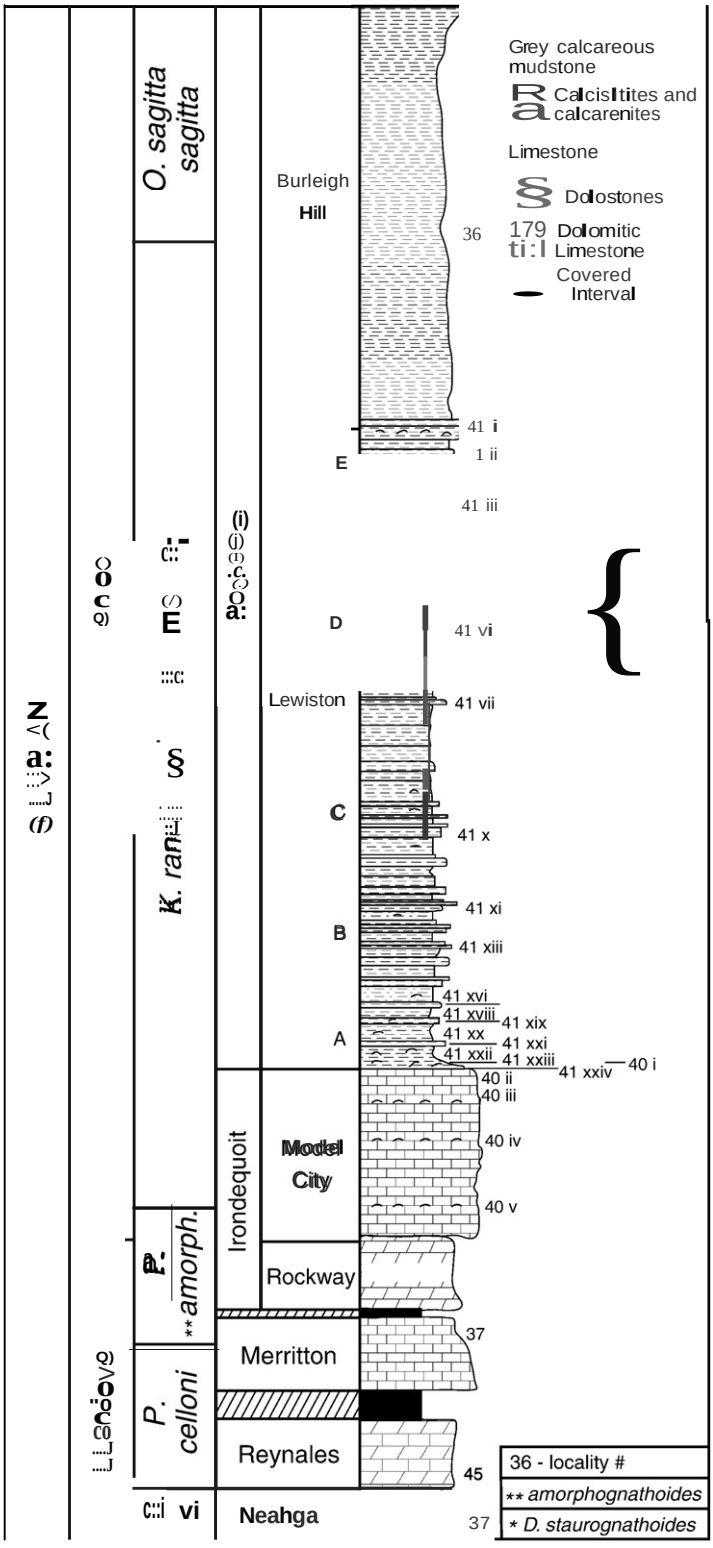

Fig. 3. Composite biostratigraphic section of the Llandovery-Wenlock interval in the Niagara Gorge area of Ontario and New York State (revised from Bates, 1990; Brett et al., 1990). Conodont zonal scheme of the section is: *Distomodus staurognathoides* (D.s.), *Pterospathodus celloni* (P *celloni*), *Pterospathodus amorphognathoides* (P *amorph.*), *Kockelella ranulifonnis-K. amsdeni*, *Ozarkodina sagitta sagitta* (0. *sagitta sagitta*), and is adopted from Rexroad and Richard (1965), Kleffuer (1989, 1991) and Johnson et al. (1998).

Varian 400 P atomic absorption spectrophotometer at Brock University with a precision and accuracy of 2.1 and 6.1%, respectively (Bates, 1990).

A subset of samples was further analyzed for carbon, oxygen and strontium isotopes (Appendix). Carbon and oxygen isotopes were corrected to a temperature of 25 °C and are reported in the standard permil notation relative to PDB. The isotope laboratories at both universities, Ottawa and Basel, claim precisions and accuracies that are better than 0.05 and 0.04‰, respectively (relative to NBS 19-IAEA).

Sample aliquots for strontium isotopes were digested in 2.5 N suprapure HCl for about 24 h at room temperature. This was followed by separation with 4.5 mL of AGW 50X8 (Biorad) cation exchange resin in quartz glass column to obtain purified Sr. The determinations were done at the Ruhr University, Bochum. Loading blank was below 5 pg, column blank was less than 1 ng, and reagent blank was below 0.01 ppb. The mean for the SRM (NBS 987) in this batch was 0.710234 ± 0.000005 (2σ). Precision of duplicate analyses was better than 0.000007. All strontium isotopes used in this paper are corrected to a nominal N.B.S. 987 value of 0.710240. For analytical details see Diener et al. (1996).

3. Sample preservation

Carbonate and phosphatic allochems that are carrier phases for tracers that serve as proxies for composition of coeval seawater must be carefully scrutinized for their physical, mineralogical and chemical preservation (cf. Brand and Veizer, 1980, 1981; Popp et al., 1986; Grossman, 1992; Brand, 2004; Lee et al., 2004). This, nevertheless, should not lead to a situation where an entire group of fossils is dismissed because a single species and/or a few specimens in a particular study may have yielded spurious results (e.g., Terebratulina, Auclair et al., 2003; Pentamerida, Samtleben et al., 2001). By the same token, it should not be automatically assumed that an entire group preserves its chemistry when a single study, based on few specimens, is at odds with complementary observations. As an example, conodonts are assumed to have retained their original seawater strontium isotope composition (Ruppel et al., 1996, 1998) despite abundant literature that documents ubiquitous diagenetic impact on biogenic apatite (Bertram et al., 1992; Cummins and Elderfield, 1994; Diener et al., 1996; Brand et al., 2004). Conodonts, even with low CAI, and other apatite fossils, often have $^{87}Sr/^{86}Sr$ ratios that are more radiogenic than their enclosing limestones (Holmden et al., 1996), suggesting a general susceptibility of biogenic apatite to post-depositional Sr exchange.

Observations by scanning electron microscopy show that the bulk of brachiopods from the entire Clinton Group is well preserved. The trabecular fibers of the secondary layer in Whitfieldella nitida and of Eospirifer radiatus are two of the many well-preserved specimens from the Lewiston Member (Fig. 4A,B). By definition, the preservation of trabecular fibres signifies the good preservation of the secondary shell layer itself (cf. Bathurst, 1975; Carpenter and Lohmann, 1995; Brand et al., 2003). Distinct trabecular fibres are also preserved in the brachiopod Resserella elegantula from the Burleigh Hill Member of the Rochester Shale (Fig. 4C). More importantly, Fig. 4D speaks for preservation of well-defined trabecular fibres also in the pentamerid Pentamerus oblongus. This is important, for recently Samtleben et al. (2001) proposed that the 'different shell succession' for Conchidium biloculare, Gypidula galeata and Kirkidium knightii exhibit large differences in their stable isotope compositions, and, thus, pentamerids as a group yield non-equilibrium isotope results and should not be used as seawater proxies. However, the "...amalgamated prismatic crystals..." in the shell of C. biloculare (Fig. 3D in Samtleben et al., 2001) appear to us to be diagenetic in origin. Evaluating their pentamerid isotope results, obviously altered ones were rejected from further consideration and using only those with sample numbers consecutive to Atrypa reticularis from formations (unfortunately no horizon information was provided by the authors to establish synchroneity of sample pairs), no differences (in ANOVA test results) were noted between the different brachiopods. Specifically, the carbon and oxygen isotope values between paired A. reticularis (+0.23‰, −5.52‰) and K. knightii (−0.28‰, −5.66‰) were not significantly different ($p = 0.294$, $p = 0.774$, respectively) at the 95% confidence level. Similarly, the carbon and oxygen isotope values of paired A. reticularis (+0.12‰, −5.47‰) and G. galeata (+0.27‰, −5.54‰) were not significantly different ($p = 0.294$, $p = 0.739$, respectively) at the 95% confidence level. Thus, their concern with not using the isotopes of brachiopods with these types of shell successions (three layers) is unfounded for pentamerids and non-substantiated by isotope results of modern counterparts with similar shell-layer morphology (Parkinson et al., 2005). In our study, pentamerids from the Merritton and Reynales Formations not only preserve their trabecular fibres but their shell lustre is similar to that in recent counterparts. Furthermore, pentamerid brachiopods from Estonia (Heath et al., 1998) have $\delta^{13}C$ and $\delta^{18}O$ values similar to other brachiopods from the same or adjacent horizons. We therefore propose that pentamerids, those with preserved secondary layer fibers, can be useful carriers of proxy

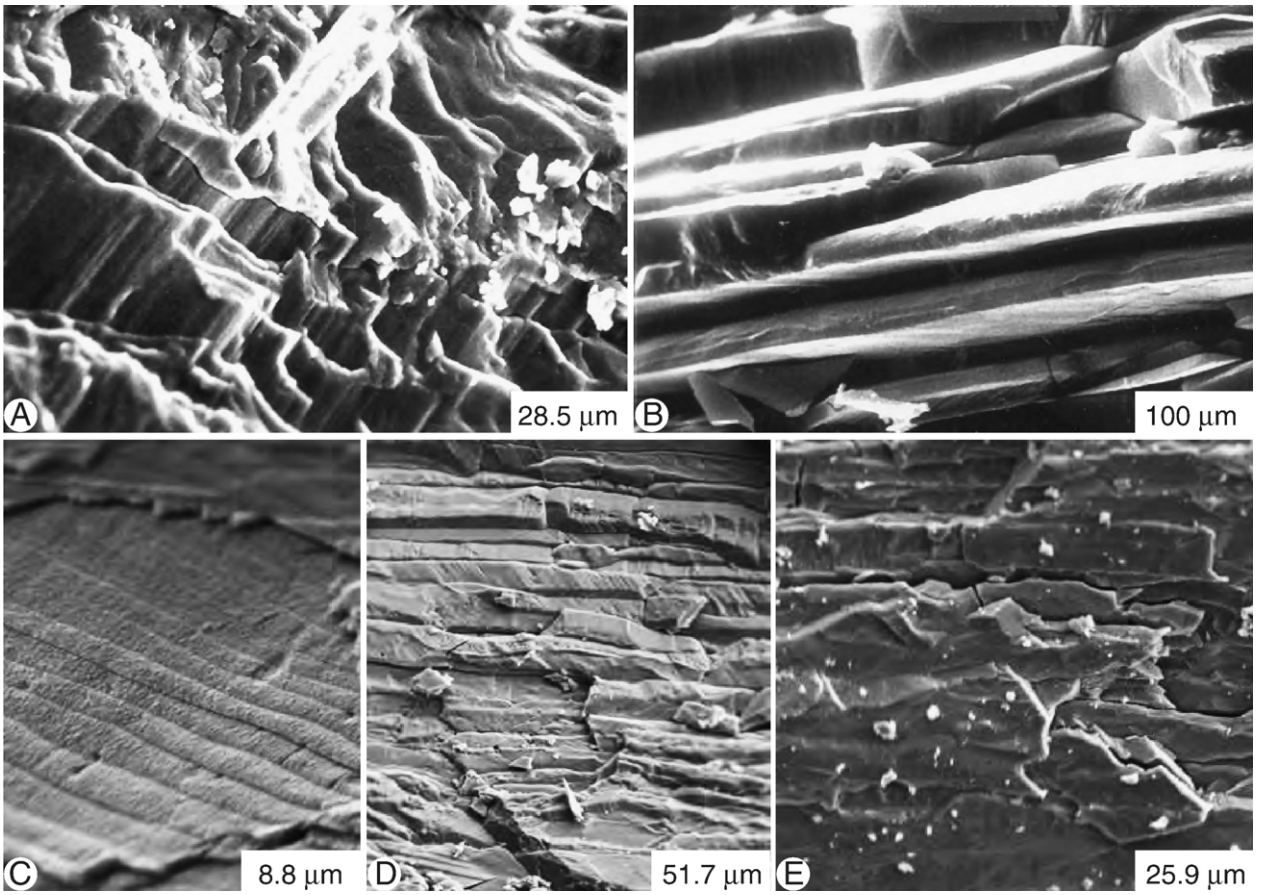

Fig. 4. Scanning electron microphotographs of internal shell structures for brachiopods (broken surfaces) from the Early Silurian Rochester, Merritton and Neagha Formations of the Niagara Gorge area. A is sample #2108 (Whitfieldella nitida, Rochester Shale) with well-preserved trabecular fibres of the secondary layer. B is brachiopod sample #2301 (Eospirifer radiatus, Rochester Shale) with well-defined trabecular fibres of the secondary shell layer. C is a surface view of trabecular fibres of sample #3014 (Resserella elegantula) from Burleigh Hill Member, Rochester Shale. D are well-defined trabecular fibres in sample #2009 (Pentamerus oblongus) from the Merritton Formation. E are slightly fused trabecular fibres in sample #N-4000 from the Neagha Formation.

signals for original seawater chemistry. We apply this interpretation to pentamerids from the Merritton and Reynales Formations (Appendix). Note that brachiopods from the Neagha Formation that show trabecular fibres in different stages of amalgamation are considered by us to have suffered some degree of diagenetic alteration and thus may not yield reliable proxy signals.

Additional criterion for preservation of the studied material is the chemical composition of the shells (Brand and Veizer, 1980; Brand, 2004). Brachiopods with low Mn and Fe and high Sr and Na contents from individual horizons are compared to their enclosing matrix in order to test for possible covariance of isotopes (Fig. 5). For $\delta^{13}C$, the results are uncorrelated, with brachiopods more positive in ten instances and more negative in five of them. For $\delta^{18}O$, the "unaltered" brachiopods have in all instances more positive values than their enclosing matrix (Fig. 5B), reflecting the greater susceptibility of the matrix to diagenetic alteration (cf. Brand and Veizer, 1981; Brand, 1991, 2004; Grossman, 1994). For the same reason, the matrix is always enriched in ^{87}Sr (Fig. 5C). Isotope values of brachiopods and matrix from the Niagara Gorge area that are deemed problematic and/or diagenetically altered (bold-faced in the Appendix) are not used in the construction of Figs. 6, 8 and 10. Unfortunately, such screening was not possible for the published data (Figs. 7, 9 and 11). Nevertheless, for construction of the composite high-resolution Sr, C and O isotope records only the 'best' results from all studies were used (Fig. 12).

4. Isotope results

Figs. 6, 8 and 10 are a compilation of Llandovery–Wenlock brachiopod data from the Niagara Gorge (Fig. 3) together with those from Anticosti Island and Gotland of Azmy et al. (1998, 1999). Correlation between these

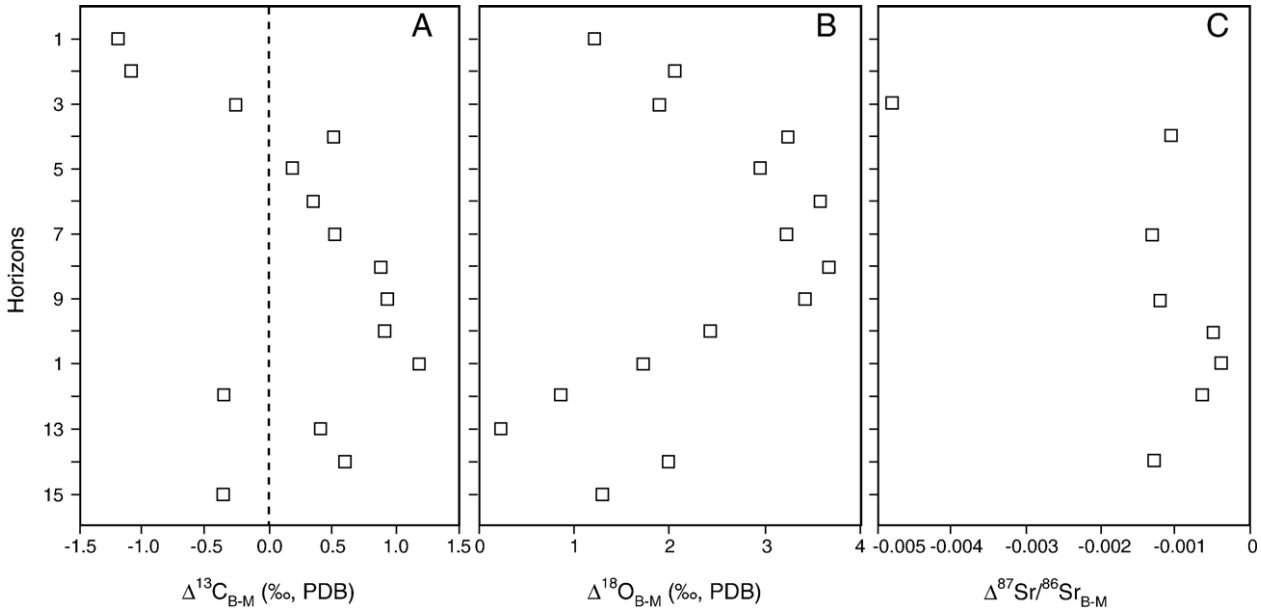

Fig. 5. The difference in average isotopic composition of the brachiopod shells and their enclosing matrix (Δ_{B-M}) for specific horizons of the Rochester (Burleigh Hill, 1, 2; Lewiston C, 3; Lewiston A, 4, 5, 6, 7, 8, 9), Irondequoit (10, 11, 12), Merritton (13), Reynales (14) and Neagha (15) Formations of the Clinton Group (Fig. 3). No trend is evident for carbon isotopes ($p = 0.712$, $N = 15$), but the matrix shows a significant depletion ($p = 0.0001$, $N = 15$) in ^{18}O and significant enrichment ($p = 0.015$, $N = 8$) in ^{87}Sr, relative to the coeval brachiopods.

various localities was achieved by using conodont zones (were given with specific boundaries), graptolite zones, and matching Sr isotope values. The sum total is the biochemostratigraphic framework as presented in Fig. 6 and subsequent ones. Figs. 7, 9 and 11 are compilations of all available data for the Llandovery–Wenlock interval. Inclusion of geochemical data from other studies was made difficult by an evolving biostratigraphy with its variations in ranges, mismatched boundaries, and different zone names just to mention a few problems encountered in trying to establish correlation between the various geochemical databases. For example in some instances, samples and results were just assigned to a formation/member, which makes stratigraphic assignment extremely difficult. The horizontal error bars (mB) represent the range of $^{87}Sr/^{86}Sr$ values observed in modern brachiopods (Brand et al., 2003), which is deemed by us to be the "natural" seawater range at any particular time. Values outside this range (e.g., A510 — 0.708161 versus A757 — 0.708079; Azmy et al., 1999) are considered altered, unless specifically proven to be pristine (cf. Brand, 1991; Brand et al., 2004). Thus in some cases, unless otherwise indicated, the size of the symbols indicates stratigraphic uncertainty (the latter applies to the data of this study and those of Azmy et al.). Ultimately Fig. 12, a composite of all available geochemical information of the studied interval, will not include data that are deemed problematic by us due to lack of stratigraphic and diagenetic information provided in their original publications, or possibly by overprinting of global seawater trends ($\delta^{13}C$, $\delta^{18}O$) by local–regional conditions. Despite these precautions it may still be possible for spurious results to have been included in the summary figure.

4.1. Strontium isotope chemostratigraphy

Strontium isotopic composition of well-preserved brachiopods from the Niagara Gorge area, as well as those from Anticosti Island, Gotland, Lithuania, Podolia and England (Azmy et al., 1999), is our proxy of choice for global correlations of Silurian sedimentary sequences (Veizer et al., 1997; Brand et al., 2003; Brand, 2004). A definitive trend of increasing $^{87}Sr/^{86}Sr$ through time is evident in Fig. 6 for the Llandovery–Wenlock interval (Fig. 6) commences with a rise in graptolite zone 8, followed by a decrease to zone 9, a steady increase through to zone 11, and a decrease to the base of zone 12. The next zone, 13, shows an increase in radiogenic strontium that is far greater than any earlier variation(s). From zone 13 through to the middle of zone 19, the strontium isotope trend is a characterized by a low-amplitude sinusoidal curve with some minor excursions (e.g., zone 16). Another sharp increase in radiogenic Sr is evident from mid-zone 19 into zone 20 (Fig. 6) and beyond (Azmy et al., 1999).

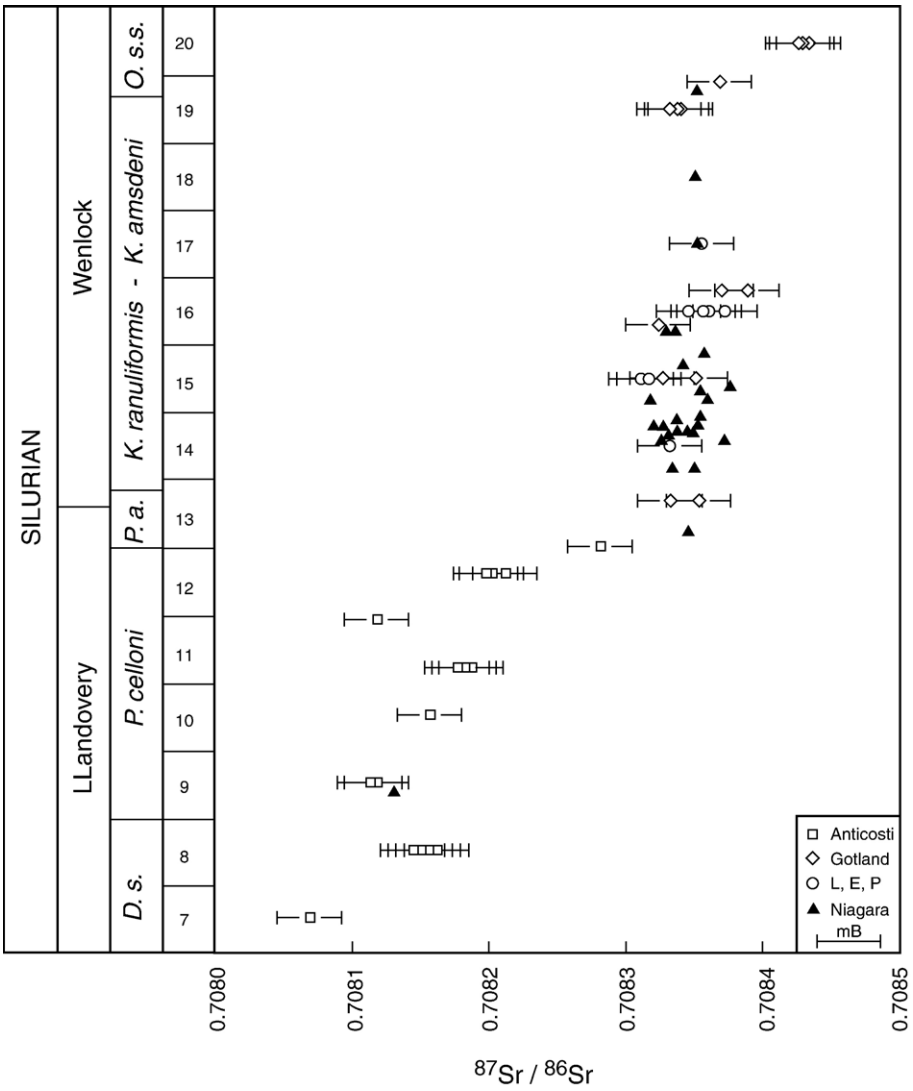

Fig. 6. Strontium isotope trend for the Llandovery–Wenlock interval based on well preserved and stratigraphically well-constrained brachiopods from the Niagara Gorge area and those from Anticosti Island, Gotland and other European localities (L — Lithuania, P — Podolia, E — England; Azmy et al., 1999). The graptolite zonation is as follows: 7, Pb. leptotheca; 8, Dm. convolutus; 9, St. sedwickii; 10, Sp. turriculatus; 11, M. crispus; 12, Mcl. grienstoniensis; 13, Mcl. crenulata; 14, Cy. centrifugus; 15, Cy. murchisoni; 16, M. riccartonensis; 17, Cy. rigidus; 18, M. flexilis; 19, Cy. ellesae; 20, Cy. lundgreni (adopted from Berry and Boucot, 1970; Jeppsson et al., 1995; Melchin et al., 1998; Azmy et al., 1999). The conodont and graptolite zonations, although in a state of flux, have been superposed to facilitate correlation of present data with those of Azmy et al. (1998, 1999). The mB represents the isotopic range observed in modern brachiopods (Brand et al., 2003).

Strontium isotope data of other sources and materials (conodonts and matrix) are compiled in Fig. 7. The matrix-based results of Denison et al. (1997), which, aside for two exceptions are always significantly more radiogenic than the brachiopod data, have very large stratigraphic uncertainty. The ^{87}Sr enrichment in these samples clearly indicates that the matrix is diagenetically altered and the measured Sr isotope ratios do not represent original seawater values (Brand, 2004). The Sr isotope results of some conodonts are also marred by a high stratigraphic uncertainty and by susceptibility to diagenetic alteration. This accounts for their more radiogenic Sr (Brand, 1991, 2004; Brand et al., 2003). Only two of the eight data points in Qing et al. (1998) fall within the range of Sr isotopes for well-preserved brachiopods (Fig. 7). Similarly, conodonts reported in Ruppel et al. (1996, 1998), while better stratigraphically assigned, show also marked diagenetic alteration. This is particularly evident for zones 7 through 10, one sample in zone 12, one in zone 14, and one in zone 19. Based on the above

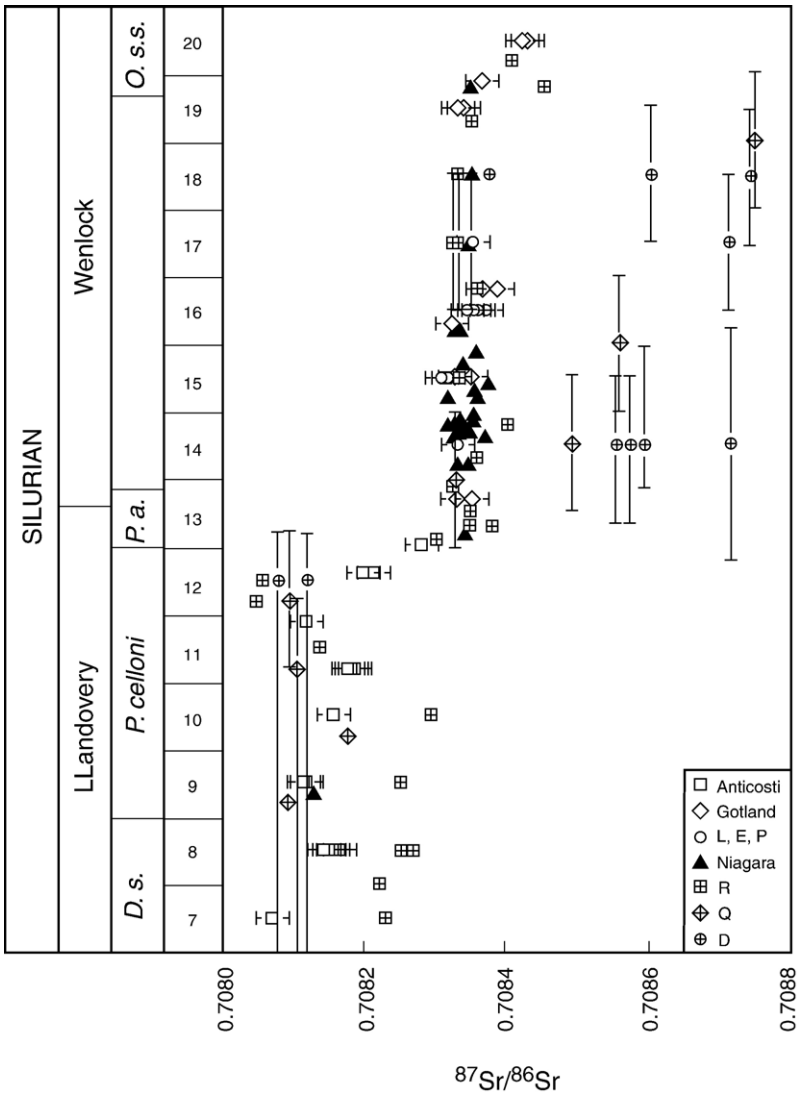

Fig. 7. Strontium isotope trend/values of well-preserved brachiopod material (Fig. 6), of matrix from other locations (D; Denison et al., 1997), as well as conodonts from Oklahoma, Tennessee, Anticosti and England (R; Ruppel et al., 1996, 1998) and from Indiana, England and Anticosti (Q; Qing et al., 1998). Vertical bars represent stratigraphic uncertainty of samples. Other information as in Fig. 6.

considerations, only the well-preserved brachiopods of this study, Azmy et al. (1999), and few acceptable conodont results are used to construct the improved high-resolution $^{87}Sr/^{86}Sr$ record for the Llandovery–Wenlock interval in Fig. 12.

4.2. Carbon isotope chemostratigraphy

The Niagara and Anticosti brachiopod-based $\delta^{13}C$ data from graptolite zones 7 through 13 exhibit values in the −0.8 to +3.1‰ range, with a mean of ~ +1.2‰ (Fig. 8). The mean $\delta^{13}C$ value for this interval is in general agreement with the post-Hirnantian value of Brenchley et al. (2003). A sharp increase of about 4‰ in the Niagara–Anticosti–Gotland data appears between graptolite zones 13 and 14 (Fig. 8), coincident with the previously cited Ireviken biotic event identified at Gotland (Jeppsson, 1987; Talent et al., 1993; Munnecke et al., 2003) and interpreted to reflect a decrease in hemi-pelagic productivity (e.g., Jeppsson, 1990, 1998). On Gotland, this event is represented by up to 13 m of faunal changes while at other localities it is marked by sudden changes within a 1 m interval (Munnecke et al., 2003). The fact that the Llandovery–Wenlock carbon isotope shift was observed in brachiopods from North America and Europe suggests a global significance of the signal.

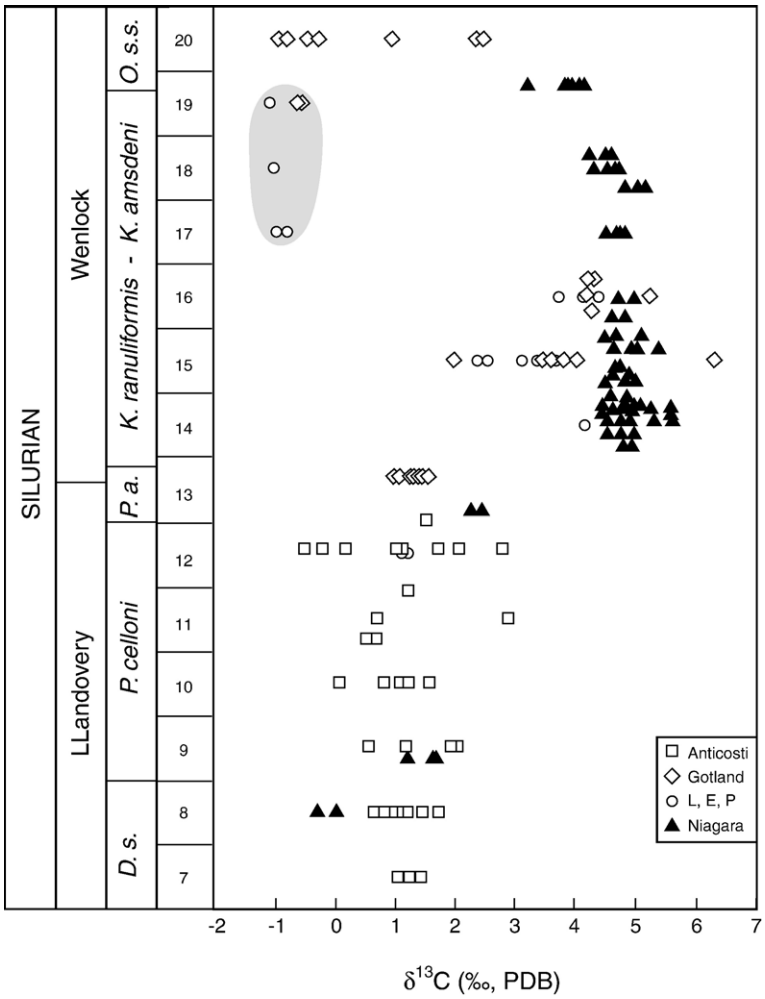

Fig. 8. Carbon isotope trend for the Llandovery–Wenlock interval based on well-preserved and stratigraphically well-constrained brachiopods from the Niagara Gorge area, and those from Anticosti Island, Gotland and other European localities (Azmy et al., 1998). Shaded area represents problematic samples (e.g., possibly diagenetically altered, uncertain stratigraphic placement, and/or other unknown factor[s]). Other information as in Fig. 6.

The large scatter of carbon isotopes during graptolite zone 15, +2 to +6.5‰ (Fig. 8), particularly for samples from Gotland and Lithuania, and the dichotomy of values for Niagara vs. Gotland and Lithuania for graptolite zones 17 through to 19 (Fig. 8) are not yet understood. The divergent $\delta^{13}C$ trends start converging again by about graptolite zone 20. This dichotomy may be an artefact of the stratigraphic correlation problems mentioned above and encountered in assigned geochemical data from other sources.

The compilation of $\delta^{13}C$ data from other sources (Fig. 9) confirms the global validity of the previously discussed $\delta^{13}C$ signal and sudden increase around the Ireviken biotic event/excursion. The post Ireviken pattern, from graptolite zone 16 to 20, is nevertheless more complex, with a suggestion of a trimodal trend. Gotland and Lithuania material have the most negative $\delta^{13}C$ values, those from Estonia, Nevada and Oklahoma are intermediate, and the Niagara Gorge samples have the heaviest ones (Fig. 9). The divergence of the intermediate trend from the "heavy" one may reflect differences in habitat water depth between Estonia (Heath et al., 1998) and the Niagara Gorge, whereas the "lighter" Gotland and Lithuania brachiopods may record warmer waters at lower latitudes (Fig. 1), combinations thereof or other oceanographic factors such as differences in seawater productivity and/or organic matter burial, or simply overprinting of 'global trends' by local/regional environmental conditions.

4.3. Oxygen isotope biochemostratigraphy

Azmy et al. (1998) discussed the multitude of parameters, such as water temperature, salinity, depth, stratification, glaciations, short- and long-term secular

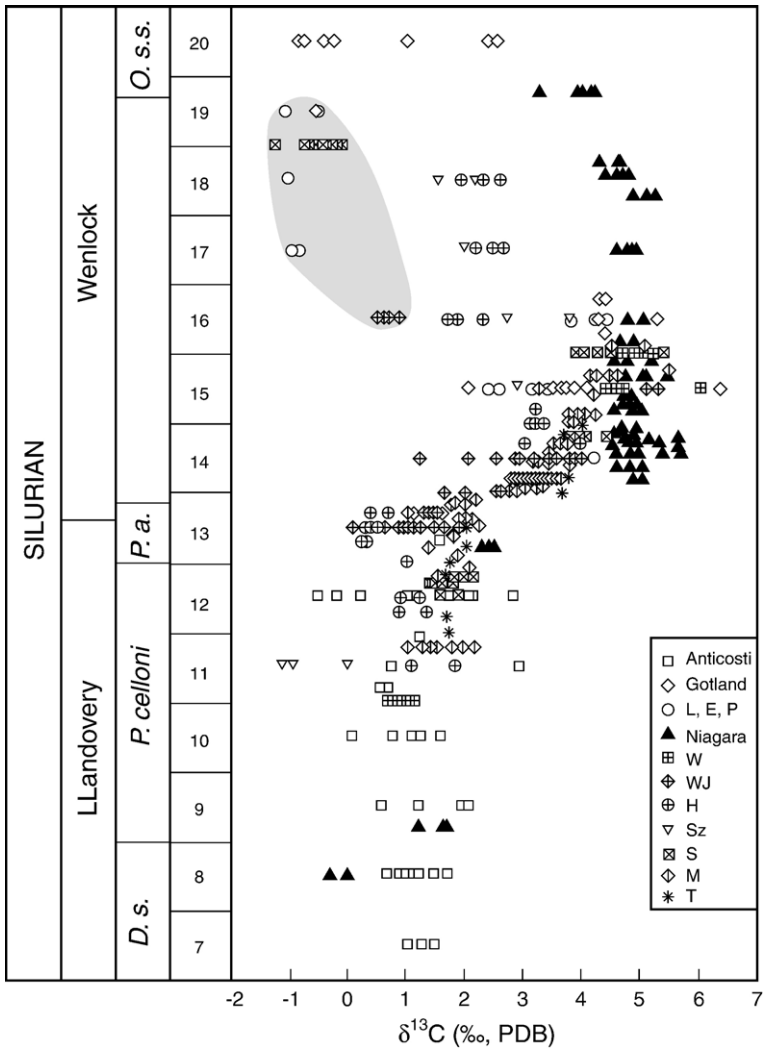

Fig. 9. Carbon isotope trend of well-preserved brachiopod material (Fig. 8) and brachiopod/matrix from other locations: Estonia (H — Heath et al., 1998), wide geographic distribution (W — Wadleigh and Veizer, 1992), Gotland (WJ — Wenzel and Joachimski, 1996; S — Samtleben et al., 2001; M — Munnecke et al., 2003), Nevada and Oklahoma (Sz — Saltzman, 2001) and New South Wales (T — Talent et al., 1993). Other information as in Figs. 6 and 8.

changes in seawater-^{18}O, that all can affect the isotopic composition of brachiopods. The brachiopod-^{18}O values during graptolite zones 7 through 11 (Niagara and Anticosti Island) range from about −4 to −5.6‰ (Fig. 10), followed by a distinct drop during zones 12 and 13 (Niagara, Anticosti Island, Gotland and Lithuania), and by a subsequent marked shift towards heavier values in zone 14. Afterwards, the δ^{18}O shifts gradually to lighter values.

A compilation of all δ^{18}O values for brachiopods and matrices (Fig. 11) reflects the same picture with minor modifications. The previously noted slight negative trend in zones 12 and 13 (Fig. 10) appears to have commenced already in the upper part of zone 11 and lasted until the lower portion of zone 14 (Fig. 11). This "trough", from −4.8 to −6.3‰, is based on brachiopods from North America (Niagara and Anticosti), Lithuania, Estonia and Gotland. The "large positive shift starts in the upper zone 14, but the spread of δ^{18}O values in zones 14 to 16 is large. Within this spread, the 'heavy' brachiopod and matrix samples are from Niagara, New York, Oklahoma/Nevada, and Estonia, and the 'light' population encompasses brachiopods from Gotland. Brachiopods from Lithuania, Podolia and England have intermediate values. The spread narrows by zone 17, and in zones 19 and 20 the δ^{18}O values decline into a range similar to zones 7 through 11 (Fig. 11).

5. Llandovery–Wenlock tectonism, oceanography and chemostratigraphy

The combined high-resolution records of seawater isotope composition should reflect tectonic, oceanographic, climatic and biotic events during the Llandovery–Wenlock transition. The tectonic history of the Appalachian Foreland Basin was considered to have been a time of relative quiescence between the Taconic and Acadian Orogenies. Recently, Ettensohn and Brett (1998) amassed convincing evidence from volcanism, plutonism, deformation and stratigraphy, complemented by observations from other continents, for at least some tectonic activity during this supposedly 'quiet' time. The stratigraphic record of the basin is divided into several sedimentary cycles by unconformities and their coincidence with the Silurian sea level fluctuations and glaciations suggests a possible global connection. The Salinic Disturbance (Boucot, 1962) coincides with the closure of the Iapetus Ocean that resulted in Caledonian consolidation of the Laurentian, Baltican, Chukotkan and Avalonian terrains into Laurussia during the Early Silurian (Ettensohn and Brett, 1998). These authors place the beginning of the 1st Salinic Disturbance into the latest Telychian and its end prior to the beginning of the 2nd Salinic Disturbance in the earliest Wenlock (Ettensohn and Brett, 1998, Fig. 8). They also proposed that the 1st tectophase was of global significance, while the 2nd tectophase was a regional event restricted to Laurussia and active only along the Caledonian suture.

Intense tectonic activity during the Late Llandovery and related subsidence appear to have coincided with a well-documented, extensive and major sea level

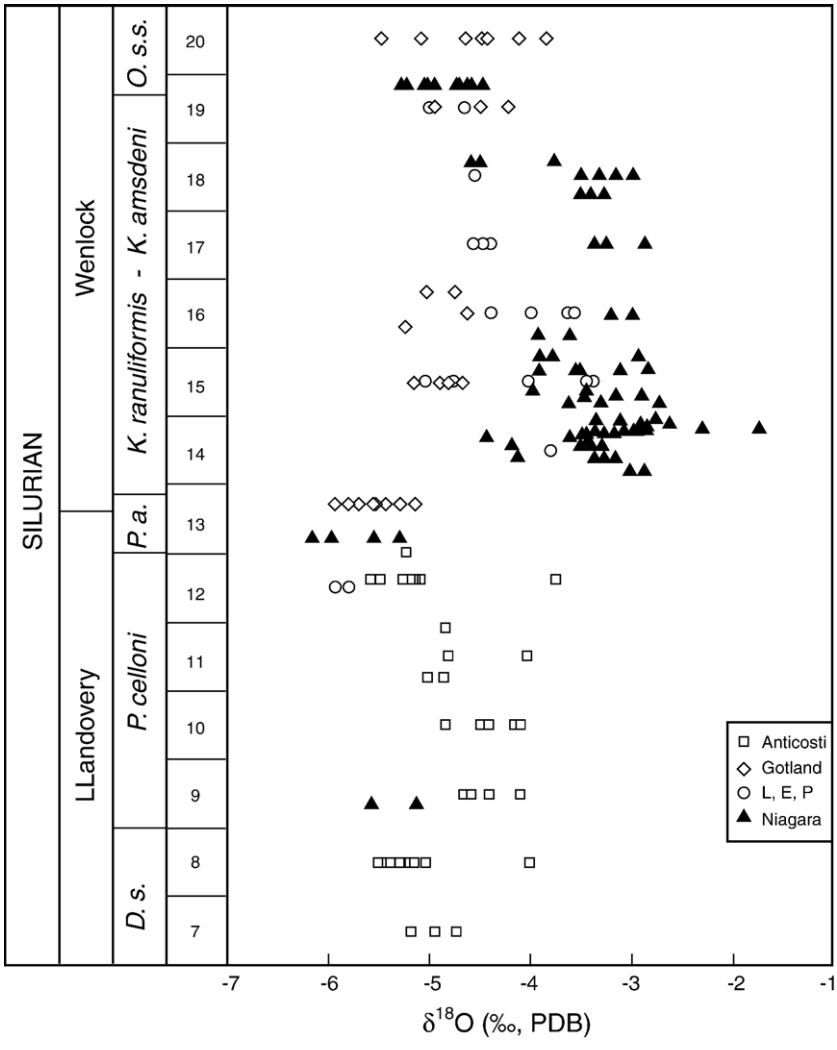

Fig. 10. Oxygen isotope trend for the Llandovery–Wenlock interval based on well-preserved and stratigraphically well-constrained brachiopods from the Niagara Gorge area, and those from Anticosti Island, Gotland and other European localities (Azmy et al., 1998). Other information as in Figs. 6 and 8.

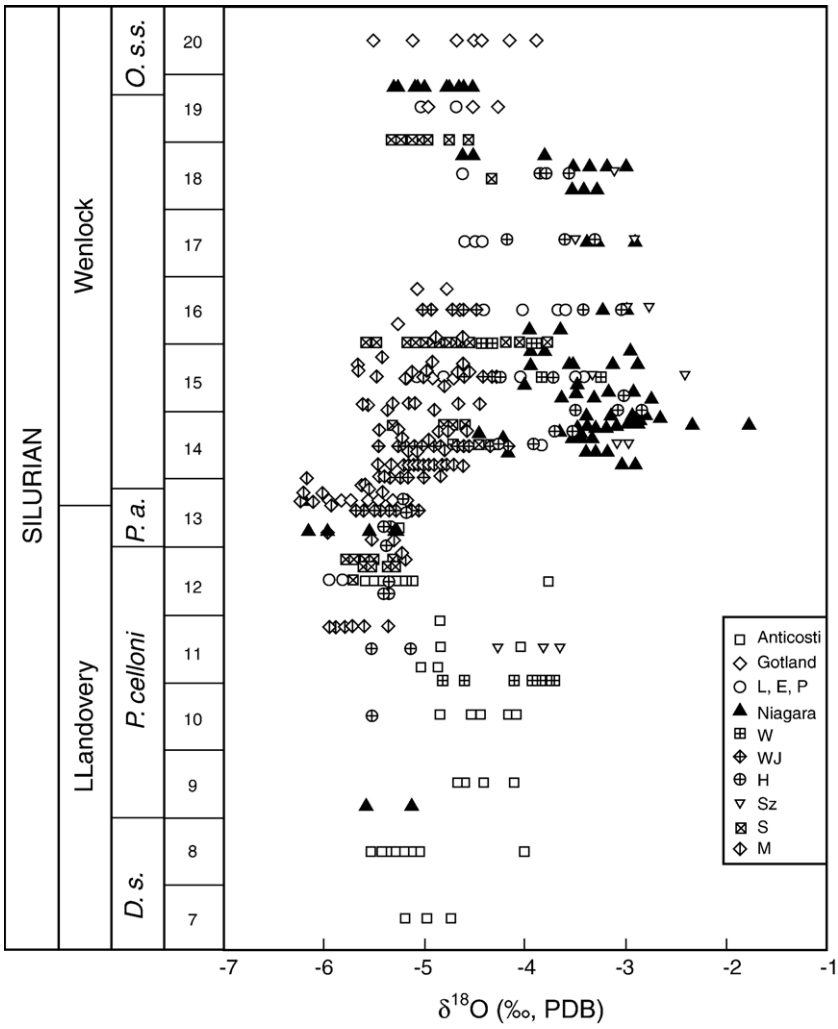

Fig. 11. Oxygen isotope trend of the Niagara Gorge, Anticosti and Gotland brachiopod material as well as data of other brachiopods and matrix from other locations (sources as in Fig. 9). Other information as in Figs. 6 and 8.

highstand, SHS (Vail et al., 1977; Scotese and Golonka, 1992; Ettensohn and Brett, 1998). Ettensohn and Brett (1998, p. 156) further suggested that this sea level highstand immediately preceded the youngest-known, 4th episode, of the Early Silurian glacial successions (Grahn and Caputo, 1992; Caputo, 1996, 1998) and that "... tectono- and glacio-eustatic components reinforced each other in the Late Telychian to produce...the maximum sea-level rise of the Silurian."

The regression following the sea level highstand appears to correspond to the Cyrtograptus lapworthi event that spans the Llandovery–Wenlock boundary (Melchin, 1994; Storch, 1995). It is further assumed that the Early Silurian glaciation was responsible for this sea level fall (Melchin et al., 1998) and that its onset was coincident, in part, with the Ireviken oceanic event (Jeppsson et al., 1995; Melchin et al., 1998) and excursion (Calner et al., 2004). Only the 'best' results of non-problematic material will be used in the construction of Fig. 12, however, it is not inconceivable that some perfectly good material may be excluded while some questionable results of sources may still be included in its construction.

5.1. Ll–W boundary-event chemostratigraphy

Isotope values of unaltered brachiopods from the Niagara Gorge area, Anticosti Island and Gotland, and some conodonts, define an improved high-resolution seawater $^{87}Sr/^{86}Sr$ record for the Llandovery–Wenlock interval (Fig. 12A) that correlates well with the tectonic events of the Early Silurian. The terminal stage of the Taconic Orogeny is witnessed in the shift in $^{87}Sr/^{86}Sr$ towards more invariant values during graptolite zone 4

(0.708052; Azmy et al., 1999), followed by a 'quiet' phase lasting into the presently studied zone 7 (0.708070). The rise to more radiogenic values from graptolite zone 7 through 13 (0.708346) corresponds well with the 1st Salinic tectophase (Fig. 12A). This trend appears to be punctuated by two incursions of non-radiogenic Sr during zones 8/9 and 11/12, due perhaps to increased flux of hydrothermal Sr (J_{OCH}; Veizer, 1989) and/or to submarine weathering (J_{OCC}). Considering the putative amplitude of $J_{OCH}1$ ($\Delta^{87}Sr = -0.000034$), hydrothermal processes could account for this dip within the available temporal constraints (Veizer, 1989, Table 1). The $J_{OCH}2$ excursion is significantly larger ($\Delta^{87}Sr = -0.000134$), and is followed by a steep Late Llandovery rise. Such large oscillations likely reflect variations in Sr flux due to continental runoff, and ultimately related to termination of the 1st Salinic tectonic event.

Hydrothermal flux of Sr from mid-oceanic ridges should be proportional to the rate of sea-floor spreading (Veizer, 1989), and high 'sea-level' stands should therefore coincide with times of fast spreading plates (Spooner, 1976; Vail et al., 1977; Elderfield, 1986), a proposition in accord with the $J_{OCH}2$ trough (Fig. 12A; Ettensohn and Brett, 1998).

The 2nd Salinic tectonic event is marked by relatively low-amplitude Sr isotope values until zone 19, with a mean of about 0.708344 ± 0.000015 ($N = 56$; Fig. 12A), supporting the proposition that the 2nd Salinic tectonic event, the Sheinwoodian, was likely not of a global nature because of its lack of impact on the Sr-isotope signal of seawater. Only in the Homerian does the signal shift from 0.708345 to 0.708430 and beyond (Azmy et al., 1999).

All $\delta^{13}C$ values of the well-preserved Llandovery brachiopods fall within the −1.0 to +3.0‰ range (Fig. 12B), similar to values in modern shallow water, low-latitude counterparts. Subsequently, the band of $\delta^{13}C$ values becomes heavier, reaching a maximum during graptolite zone 15, particularly in the Niagara Gorge (+6.0‰) and at Gotland (+6.37‰). As already pointed out, the Ireviken event/excursion is recorded at Gotland (Munnecke et al., 2003; Calner et al., 2004), Estonia (Heath et al., 1998) and the Niagara Gorge area (Fig. 13B), and is therefore of global significance.

Such positive C-isotope excursions in the geologic record were often claimed to have been coincident with mass extinction events (e.g., Saltzman et al., 1998; Brenchley et al., 2003; Brand et al., 2004). However, similar large $\delta^{13}C$ excursions during the Early to Mid-Paleozoic were recorded also in the latest Hirnantian (Marshall et al., 1997; Brenchley et al., 2003), Late Ludlow (Azmy et al., 1998) and the latest Famennian (Brand et al., 2004). In the Baltic Hirnantian, the positive carbon isotope excursion commenced at about the same time as the onset of glaciation (Brenchley et al., 1994, 2003) and a similar pattern was noted also for the latest Famennian of Europe and North America (e.g., Brand et al., 2004). In both cases, the $\delta^{13}C$ reverted back to almost pre-event values after the event. The coincidence of the Ireviken event and excursion, the $\delta^{13}C$ positive excursion, and the cooling connected to the Cancañiri glaciation (Fig. 12) permits similar interpretation also for the present dataset.The post maximum band appears to have been bimodal (Fig. 12B) up to at least zone 20. The lighter values (~ −1.0‰) are mostly from Gotland samples and from Estonia (Heath et al., 1998; ~ +2.0‰), the latter from a somewhat deeper habitat. The heavy (~ +4.5‰) branch is mostly the samples from the Niagara Gorge. In summary, the increase in the $\delta^{13}C$ of well-preserved brachiopods during graptolite zone 14 is of a global nature and can be utilised for correlation purposes.

Oxygen isotope values of unaltered brachiopods from a multitude of locations define a trend that, in part, mimics the one for carbon isotopes (Fig. 12C), but the $\delta^{18}O$ increase postdates the rise in Sr isotopes. As for carbon isotopes, this suggests that tectonics was not the imminent causative factor. Note that the spread of $\delta^{18}O$ values for the Llandovery–Wenlock brachiopods is similar to that in modern shallow-water, low-latitude counterparts (Fig. 12C), but the entire band is shifted to a depleted $\delta^{18}O$ range, by ~ 3‰ (Figs. 12C and 13). The observed spread of $\delta^{18}O$ within the band, as in modern samples, can readily be explained by differences in location, oceanographic configuration (basin size and morphology), water depth, salinity, currents, storms and particularly by glacial/non-glacial conditions (Lécuyer and Allemand, 1999; Wallmann, 2001). For example, samples from the Estonian Ruhnu core (Heath et al., 1998) are enriched in ^{18}O relative to other locations within Baltica (Azmy et al., 1998) due to their origin from a "...deep-shelf environment..." of at least "...200 m..." (Heath et al., 1998; p. 314, 320). As seen from modern examples (Fig. 13) the assumed greater depth, by about 100 to 150 m relative to the other Baltic samples, can easily account for the $\delta^{18}O$ variability of about 2‰ in the $\delta^{18}O$ band. However, the offset of ~ 3‰ between Silurian and modern brachiopods requires a different explanation.

During the earliest Llandovery, $\delta^{18}O$ values of brachiopods vary from −5.4 to −3.7‰ (Fig. 12C), but at the end of graptolite zone 11, the $\delta^{18}O$ values dip by about 1.4‰, and range from −6.9 to −5.1‰. This global 'light'

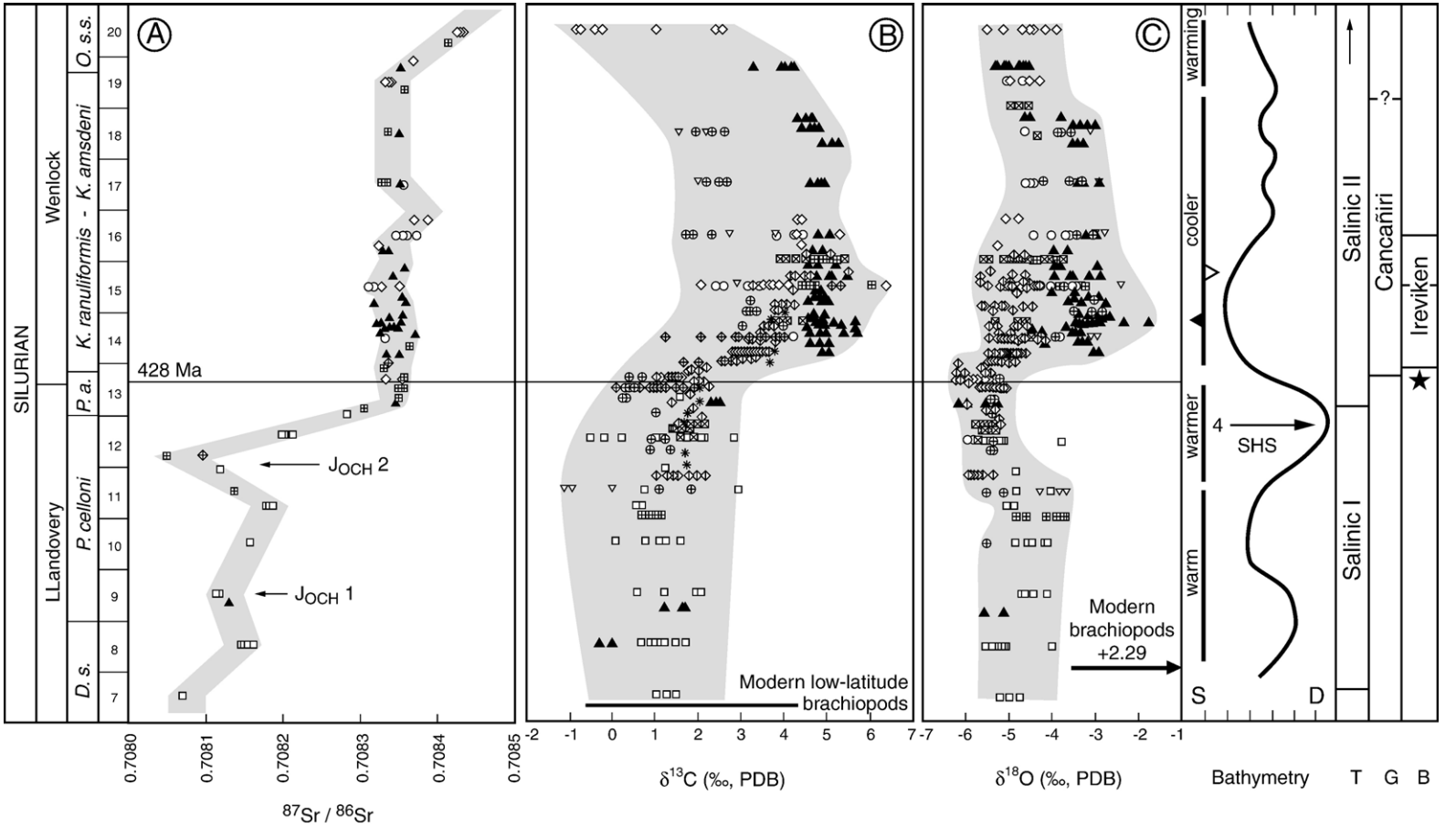

Fig. 12. Summary diagram of high-resolution isotope trends (strontium [A], carbon [B] and oxygen [C]) for the Llandovery–Wenlock interval using only the 'best' of all materials. Marked also are the tectonic (T) events Salinic I/part II (Ettensohn and Brett, 1998), glacial (G) Cancañiri episode (Hambry, 1985; Grahn and Caputo, 1992; Caputo, 1998) and biotic (B) Ireviken event and excursion (Walliser, 1964; Jeppsson, 1987, 1998; Talent et al., 1993; Munnecke et al., 2003; Calner et al., 2004). The sea level changes in bathymetry are: S — shallow, D — deep (Johnson, 1996; Johnson et al., 1998) and SHS — Silurian highstand (Ettensohn and Brett, 1998). The age for the Llandovery–Wenlock boundary is from Tucker and McKerrow (1995). The star (★) represents the Llandovery–Wenlock Cyrtograptus lapworthi boundary event (Melchin et al., 1998). J^1_{OCH} and J^2_{OCH} are the postulated hydrothermal fluxes '1' and '2'. $\delta^{13}C$ and $\delta^{18}O$ ranges for modern shallow-water, low latitude brachiopods are from Brand et al. (2003).

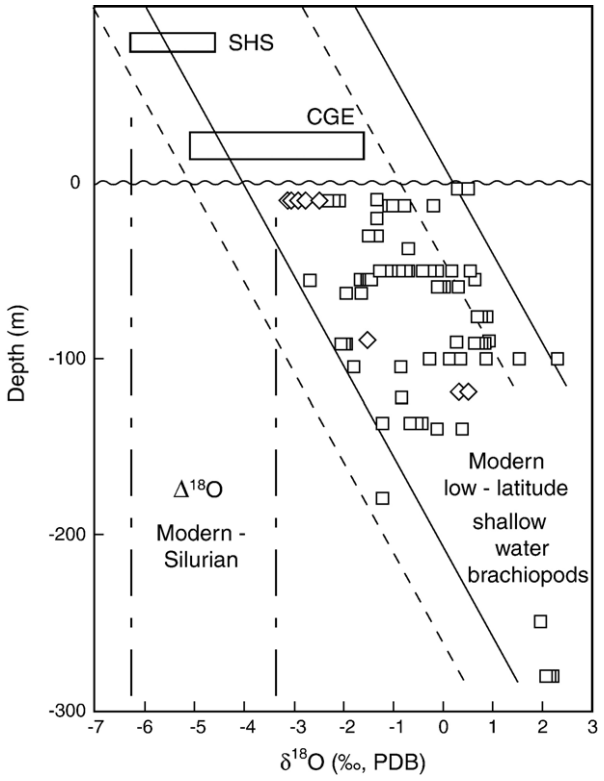

Fig. 13. Oxygen isotope values in modern shallow-water and low-latitude brachiopods vs. water depth. SHS: Silurian highstand range, and CGE: Cancañiri glacial event. The offset of isotope trend with depth for the Early Silurian represents the correction for the Phanerozoic secular trend (Veizer et al., 1999).

isotope episode coincides with the highstand of Silurian sealevel and thus a warm climatic interval. Assuming modern values for Silurian seawater (Muehlenbachs, 1998), the calculated paleotemperatures would be unreasonably high, up to 52 °C. In order to obtain "reasonable" paleotemperatures, one needs to assume the absence of any glaciation and glacial ice, giving an ice volume effect of ~ 1.2‰, plus differences in ocean salinity (cf. Lécuyer and Allemand, 1999). Moreover, the seas of zones 12 and 13 would have to been ~ 5 °C warmer than the rest of the Llandovery, a claim already made for Estonia by Heath et al. (1998; p.320). Alternatively, the general offset may result from secular evolution of seawater-^{18}O (Veizer et al., 1999).

The sealevel lowstand (base of graptolite zone 14 through to zone 16) is marked by a wide spread in δ^{18}O values, with most brachiopods from Gotland and Britain in the −5.8 to −3.7‰ range, and Niagara Gorge and Estonia in the −4.0 to −1.7‰ range. This dichotomy can, in part, be ascribed to differences in latitudes (Fig. 1). Gotland, Britain and Estonia at ~ 10°S were awash in warm equatorial currents of the Panthalassa Ocean, whereas North America, including the Niagara Gorge area, was influenced by storms and cold currents from the Gondwana continent (Fig. 1) that was glaciated at higher latitudes (Hambry, 1985; Grahn and Caputo, 1992; Caputo, 1998). This 4th glacial event (Grahn and Caputo, 1992), characterized by the widespread sediments of the Cancañiri Formation of South America (Harland et al., 1982; Hambry, 1985), may have lasted from the termination of the Silurian sea level highstand until the end of graptolite zone 17 or, based on δ^{18}O values, until about the end of zone 18 (Fig. 12C). From graptolite zone 17, the δ^{18}O values of brachiopods from various localities converge to values similar to those recorded during the Early Llandovery.

6. Conclusions

Stratigraphically well-constrained and well-preserved brachiopods were used to delineate the biochemostratigraphy of the Early Silurian sequence in the Niagara Gorge area and compare/correlate it with counterparts from Anticosti Island, Britain, Gotland and Estonia. These datasets yield the following conclusions:

1) High-resolution stratigraphic trends for δ^{13}C, δ^{18}O and ^{87}Sr/^{86}Sr, based on unaltered brachiopods, record the isotopic composition of Early Silurian seawater. The combined ^{87}Sr/^{86}Sr data from North America (Niagara Gorge, Anticosti Island) and Europe (Britain, Gotland and Estonia) depict an isotopic trend that mirrors a major tectonic event, the Salinic I tectophase. The Sr isotope curve rises from 0.708070 in graptolite zone 7 to 0.708346 at the termination of the event in zone 13. The Salinic II tectophase is not well recorded in the Sr isotope record, either due to its regional nature or to overprinting by more dominant phenomena.
2) Carbon isotopes from all localities are relatively invariant for the latest Llandovery, but just inside the Wenlock boundary a large positive excursion marks the Ireviken biotic event/excursion of the Early Silurian, perhaps a response to the onset of the Cancaniri glaciation 4th episode. The post-Ireviken δ^{13}C band becomes complicated by its bi- to trimodal pattern that is not yet understood.
3) The "Silurian sea level highstand" is faithfully recorded in oxygen isotopes from all discussed locations, rapidly followed by a change to heavier δ^{18}O values, likely a reflection of cooling and sea level drop associated with the Cancañiri glacial

event. The width of the band of $\delta^{18}O$ values is to some degree a reflection of differences in the paleogeographic distribution. Brachiopods from close to the paleoequator (Estonia, Gotland, Britain) were awash in warm waters of the Panthalassa ocean, while those from the Niagara Gorge area were influenced by cold currents from, at all times, glaciated Gondwana. The $\delta^{18}O$ of all Llandovery–Wenlock brachiopods are depleted by ~ 3‰ relative to their modern counterparts. Whether this overall shift of the band is due to secular evolution of seawater-^{18}O (Veizer et al., 1999) or to a combination of specific circumstances (temperature, depth, salinity, ice volume) cannot be resolved unequivocally with this present dataset.

Acknowledgements

We thank Nick Bates for his exploratory fieldwork, collections, some analytical work, and use of his results (Bates, 1990), Mike Lauzon for drafting of figures, and Mr. D.M. Wilson (Trillium Railway Co. Ltd) for permission to access the railroad cut near Lock 5, sample location # 37 on his property. The editor, Finn Surlyk, and two anonymous reviewers have our appreciation for their incisive comments on the first draft. The authors acknowledge the Natural Sciences and Engineering Research Council of Canada (NSERC) for its continued financial support of Discovery Grants to UB and JV.

Appendix A. Geochemical data of brachiopods, matrix from lower Paleozoic Formations (Silurian) of southern Ontario, Canada (Niagara Gorge) and western New York State, U.S.A. (Sr isotope data adjusted to a nominal NBS 987 value of 0.710240; Strat Loc. = stratigraphic location [sai[Figs. 2 and 3]; a/b base: cm above/below base of Rochester Shale; IR = insoluble residue [non-carbonate fraction, Brand and Veizer, 1980]; sample isotope values in bold are deemed problematic and/or diagenetically altered)

Sample #	Formation member	Allochem	Strat loc.	a/b base (cm)	IR (%)	Mg (mg/kg)	Fe (mg/kg)	Mn (mg/kg)	Sr/Mn	$\delta^{18}O$ (‰)	$\delta^{13}C$ (‰)	$^{87}Sr/^{86}Sr$
B-3001	Rochester	Coolinia subplana	36	1320	6.20	4100	1185	280	6.27	−5.02	4.15	
B-3001d	Burleigh Hill	Coolinia subplana	36	"						−5.26	3.97	
B-3003	"	Coolinia subplana	36	"	10.60	5820	1300	270	7.09	−5.23	3.91	
B-3005	"	Leptaena rhomboidalis	36	"	8.60	7660	1060	240	11.44	−5.06	4.02	
B-3006	"	Leptaena rhomboidalis	36	"	11.20	9825	1505	410	8.14			
B-3011	"	Dalejina sp.	36	"	13.70	3610	470	180	8.88	−5.05	4.16	
B-3014	"	Resserella elegantula	36	"	6.60	4960	610	175	15.34	−4.57	3.90	
B-3015	"	Resserella elegantula	36	"	6.60	4070	550	215	12.79			
B-3016	"	Resserella elegantula	36	"	3.80	5400	790	190	13.74	−4.73	4.03	
B-3017	"	Dalejina sp.	36	"	8.50	8775	1170	270	9.44			
B-3018	"	Dalejina sp.	36	"	5.90	3390	660	120	22.66	−4.61	4.00	
B-3018d	"	Dalejina sp.	36	"						−4.57	4.01	
B-3019	"	Dalejina sp.	36	"	9.60	8770	1170	270	9.44			
B-3021	"	Coolinia subplana	36	"	10.70	10,080	1570	360	7.61			
B-3027	"	Resserella elegantula	36	"	4.50	5190	535	210	11.88	−4.96	4.21	
B-3000	"	Coolina subplana	36	"						−4.47	3.28	0.708352
B-3033m	"	Matrix	36	"	35.90	27,120	5340	850	0.15	**−6.08**	5.14	
B-3034m	"	Matrix	36	"	24.00	22,427	4230	1140	0.17	**−6.90**	5.03	
R-2530	Rochester	Resserella elegantula	41i	920	10.30	9250	1000	420	2.69			
R-2531	Lewiston E	Resserella elegantula	41i	"	6.40	5750	605	385	3.13	−4.49	4.61	
R-2533	"	Resserella elegantula	41i	"	4.20	7780	765	420	2.69	−4.59	4.65	
R-2532	"	Resserella elegantula	41i	"	11.60	12,860	1240	425	2.41			
R-2534	"	Whitfieldella nitida	41i	"	7.10	9860	1035	260	4.27	−3.76	4.30	0.708412
R-2520	Rochester	Eospirifer radiatus	41ii	900	7.70	7265	685	190	6.78	−3.48	4.79	
R-2520d	Lewiston E	Eospirifer radiatus	41ii	"						−3.13	4.62	
R-2521	"	Whitfieldella nitida	41ii	"	7.80	1540	110	65	19.00	−2.97	4.38	
R-2524	"	Eospirifer radiatus	41ii	"	6.50	2175	175	90	13.78	−3.32	4.72	0.708352
R-2545	Rochester	Eospirifer radiatus	41iii	825	7.50	1905	210	95	13.68	−3.39	5.13	

Appendix A (continued)

Sample #	Formation member	Allochem	Strat loc.	a/b base (cm)	IR (%)	Mg (mg/kg)	Fe (mg/kg)	Mn (mg/kg)	Sr/Mn	$\delta^{18}O$ (‰)	$\delta^{13}C$ (‰)	$^{87}Sr/^{86}Sr$
R-2545d	Lewiston E	Eospirifer radiatus	41iii	"						−3.49	5.23	
R-2546	"	Eospirifer radiatus	41iii	"	4.40	1985	775	210	5.90	−3.26	4.90	
R-2510	Rochester	Eospirifer radiatus	41vi	665	2.80	2140	190	70	17.00	−2.85	4.91	
R-2510d	Lewiston D	Eospirifer radiatus	41vi	"						−2.87	4.75	
R-2511	"	Eospirifer radiatus	41vi	"	8.70	2625	275	95	12.68	−3.35	4.76	0.708352
R-2513	"	Eospirifer radiatus	41vi	"	7.10	4780	580	225	4.97	−4.50	4.85	
R-2512	"	Eospirifer radiatus	41vi	"	3.70	3100	445	170	7.15	−3.25	4.60	
R-2500	Rochester	Striispirifer niagarense	41vii	400	2.60	1670	135	60	22.33	−3.19	5.05	
R-2501	Lewiston C	Striispirifer niagarense	41vii	"	3.30	2610	350	110	11.59	−2.97	4.78	
R-2462	Rochester	Whitfieldella nitida	41x	342	7.10	6620	450	140	8.71			
R-2463	Lewiston C	Striispirifer niagarense	41x	"	9.60	1930	110	110	11.95	−3.61	4.67	0.708331
R-2464	"	Striispirifer niagarense	41x	"	3.90	2140	165	80	15.38	−3.92	4.88	0.708337
R-2465	"	Striispirifer niagarense	41x	"	5.00	2575	175	75	16.40			
R-2466 m	"	Matrix	41x	"						−5.66	5.04	0.713134
R-2495	Rochester	Atrypa reticularis	41xi	233	3.30	2740	220	240	5.58			
R-2496	Lewiston B	Atrypa reticularis	41xi	"	10.30	3630	390	805	1.37	−3.91	4.54	
R-2498	"	Atrypa reticularis	41xi	"	6.10	3975	545	420	2.83	−3.78	4.76	
R-2497	"	Atrypa reticularis	41xi	"	10.20	3720	245	110	11.27	−2.92	5.16	0.708359
R 2472	Rochester	Eospirifer radiatus	41xiii	173	5.60	2680	225	140	8.57	−3.91	5.46	
R-2473	Lewiston B	Eospirifer radiatus	41xiii	"	5.40	2790	190	90	13.88	−2.84	4.73	
R-2474	"	Eospirifer radiatus	41xiii	"	9.50	2240	140	80	15.18	−3.53	5.10	0.708343
R-2474d	Rochester	Eospirifer radiatus	41xiii	173						−3.49	4.99	
R-2471	Lewiston B	Atrypa reticularis	41xiii	"	2.90	2980	380	160	7.22	−3.10	4.68	
R-2470	"	Atrypa reticularis	41xiii	"	8.30	3460	325	160	7.90			
R-2400	Rochester	Atrypa reticularis	41xvi	112	5.80	3710	300	480	2.33	−3.97	4.72	
R-2401	Lewiston B	Atrypa reticularis	41xvi	"	5.30	3890	310	160	8.00	−3.44	4.82	0.708377
R-2402	"	Atrypa reticularis	41xvi	"	6.40	4125	420	320	3.59			
R-2403	"	Atrypa reticularis	41xvi	"	10.60	4320	370	190	6.89			
R-2404	"	Atrypa reticularis	41xvi	"						−2.92	4.46	
R-2380	Rochester	Eospirifer radiatus	41xviii	90	11.10	3800	225	110	11.14	−3.14	4.83	0.708356
R-2382	Lewiston A	Atrypa reticularis	41xviii	"	10.30	4010	310	270	4.44	−3.45	4.94	
R-2383	"	Atrypa reticularis	41xviii	"	13.90	3910	360	330	2.59			
R 2385	"	Atrypa reticularis	41xviii	"	8.10	3685	230	100	12.10			
R 2387	"	Atrypa reticularis	41xviii	"	3.90	2875	280	200	5.98	−2.89	5.68	
R-2371	Rochester	Atrypa reticularis	41xix	72	13.20	3815	330	260	4.27			
R-2375	Lewiston A	Whitfieldella nitida	41xix	"	7.40	7760	470	50	22.20			
R-2377	"	Eospirifer radiatus	41xix	"	5.30	1960	110	40	34.00	−3.61	4.56	0.708362
R-2377d	"	Eospirifer radiatus	41xix	"	5.30					−3.28	4.88	
R-2378	"	Eospirifer radiatus	41xix	"	8.80	3220	235	140	9.17	−2.71	5.02	0.708321
R-2379m	"	Matrix	41xix	"						−6.43	4.31	0.709406
R-2350m	Rochester	Matrix	41xx	45						−6.01	4.58	
R-2352	Lewiston A	Whitfieldella nitida	41xx	"	6.60	7015	415	220	6.61			
R-2353	"	Whitfieldella nitida	41xx	"	6.80	3605	215	50	27.20	−2.76	4.91	0.708356
R-2354	"	Whitfieldella nitida	41xx	"	8.30	5295	460	110	13.63	−3.35	4.71	
R-2355	"	Atrypa reticularis	41xx	"	12.00	3680	285	100	13.60	−3.10	4.68	
R-2356	"	Atrypa reticularis	41xx	"	15.30	4970	430	70	22.29			
R-2341	Rochester	Whitfieldella nitida	41xxi	30	5.50	1880	140	10	117.00	−2.89	4.83	0.708339

(continued on next page)

Appendix A (continued)

Sample #	Formation member	Allochem	Strat loc.	a/b base (cm)	IR (%)	Mg (mg/kg)	Fe (mg/kg)	Mn (mg/kg)	Sr/Mn	$\delta^{18}O$ (‰)	$\delta^{13}C$ (‰)	$^{87}Sr/^{86}Sr$
R-2342	Lewiston A	Whitfieldella nitida	41xxi	"	8.30	8230	740	490	1.98	−2.61	4.77	
R-2343	"	Whitfieldella nitida	41xxi	"						−4.06	4.67	
R-2344	"	Whitfieldella nitida	41xxi	"	13.10	4855	330	170	9.11			
R-2346	"	Eospirifer radiatus	41xxi	"	5.60	2830	295	140	9.50			
R-2320	Rochester	Eospirifer radiatus	41xxiii	18	7.60	4940	315	170	6.91	−2.89	4.52	
R-2322	Lewiston A	Eospirifer radiatus	41xxiii	"	2.70	1205	115	30	38.83	−2.30	4.89	
R-2324	"	Whitfieldella nitida	41xxiii	"	5.80	2460	70	50	24.50	−2.87	4.88	
R-2323	"	Eospirifer radiatus	41xxiii	"	4.50	1335	70	35	35.43	−2.83	4.77	0.708355
R-2327	"	Atrypa reticularis	41xxiii	"	9.60	4690	365	175	7.34			
R-2328	"	Atrypa reticularis	41xxiii	"	10.00	3670	330	165	7.00			
R-2329m	"	matrix	41xxiii	"						−6.31	4.43	
R-2100	Rochester	Eospirifer radiatus	40i	12	3.60	1090	30	19	66.31	−1.74	5.15	0.708322
R-2101	Lewiston A	Eospirifer radiatus	40i	"	2.60	1735	175	75	15.93	−2.84	5.64	0.708329
R-2103m	"	Matrix	40i	"	36.20	30,650	5050	1450	0.15	−6.67	4.09	0.709635
R-2108	"	Whitfieldella nitida	40i	"	5.60	2120	230	75	15.80	−2.94	4.80	
R-2109	"	Whitfieldella nitida	40i	"	2.40	3350	385	110	10.54	−2.94	4.50	
R-2102	"	Eospirifer radiatus	40i	"	2.60	3745	485	195	6.20	−3.51	4.70	
R-2104	"	Eospirifer radiatus	40i	"	2.70	3060	295	165	6.48	−3.06	5.07	
R-2105	"	Eospirifer radiatus	40i	"	2.20	3875	370	190	6.47	−2.97	5.03	
R-2106	"	Eospirifer radiatus	40i	"	3.10	2350	280	140	8.07	−3.34	5.16	
R-2107	"	Whitfieldella nitida	40i	"						−3.74	4.67	
R-2108m	"	Matrix	40i	"						−6.23	4.45	
R-2300	Rochester	Eospirifer radiatus	41xxiv	5	14.50	1670	90	35	36.00	−3.25	5.32	
R-2301	Lewiston A	Eospirifer radiatus	41xxiv	"	4.60	3240	150	90	12.11	−3.46	4.98	
R-2304	"	Whitfieldella nitida	41xxiv	"	6.90	5225	330	205	6.05	−3.16	4.82	0.708339
R-2306	"	Atrypa reticularis	41xxiv	"	7.10	5160	375	215	5.67			
R-2308	"	Atrypa reticularis	41xxiv	"	5.70	3975	320	220	5.55	−3.43	4.70	0.708347
R-2309m	"	Matrix	41xxiv	"						−6.74	4.03	0.709549
I-2190	Irondequoit	Whitfieldella nitida	40ii	−3	3.00	1320	90	80	15.25			
I-2191	"	Atrypa reticularis	40ii	"	6.70	6720	490	360	3.13	−4.43	4.52	0.708351
I-2193	"	Atrypa reticularis	40ii	"	4.20	2970	225	115	10.26	−3.42	4.95	0.708333
I-2192m	"	Matrix	40ii	"						−6.25	4.14	0.708819
I-2194	"	Atrypa reticularis	40ii	"	11.10	22,020	2230	1390	0.63			
I-2195	"	Atrypa reticularis	40ii	"	12.50	2860	210	120	10.75	−3.61	5.65	
I-2172	Irondequoit	Atrypa reticularis	40iii	−10	9.20	3670	400	340	3.25			
I-2174	"	Eospirifer radiatus	40iii	"	15.00	5280	380	310	3.89	−4.17	4.58	
I-2176	"	Eospirifer radiatus	40iii	"	11.30	1880	135	140	9.11	−3.29	5.36	
I-2176d	"	Eospirifer radiatus	40iii	"						−3.49	5.68	
I-2173	"	Atrypa reticularis	40iii	"	8.70	1990	250	180	6.22	−4.91	4.96	0.708328
I-2182	"	Whitfieldella nitida	40iii	"	8.00	15,520	1280	930	1.08			
I-2183	"	Whitfieldella nitida	40iii	"	6.50	4850	400	375	3.15	−3.40	4.81	0.708373
I-2178m	"	Matrix	40iii	"						−5.55	3.90	0.708745
I-2131	Irondequoit	Whitfieldella nitida	40iv	−100	3.00	4040	385	240	4.31	−3.36	4.60	
I-2132	"	Whitfieldella nitida	40iv	"	7.30	4050	385	220	4.32	−4.13	4.80	
I-2134	"	Whitfieldella nitida	40iv	"	4.80	4070	200	280	3.99	−3.15	5.03	
I-2133	"	Whitfieldella nitida	40iv	"						−3.25	4.82	
I-2138	"	Whitfieldella nitida	40iv	"	6.10	6685	610	585	1.73			
I-2160	Irondequoit	Whitfieldella nitida	40v	−220	6.80	2890	150	215	5.77			
I-2161	"	Whitfieldella nitida	40v	"	5.70	2370	130	165	7.33			
I-2162	"	Whitfieldella nitida	40v	"	5.30	1555	50	70	15.78	−3.00	4.87	0.708350
I-2163	"	Whitfieldella nitida	40v	"	6.50	1945	60	110	10.63			
I-2164	"	Whitfieldella nitida	40v	"	4.70	2055	50	80	14.19	−2.87	5.00	0.708335

Appendix A (continued)

Sample #	Formation member	Allochem	Strat loc.	a/b base (cm)	IR (%)	Mg (mg/kg)	Fe (mg/kg)	Mn (mg/kg)	Sr/Mn	$\delta^{18}O$ (‰)	$\delta^{13}C$ (‰)	$^{87}Sr/^{86}Sr$
I-2162m	"	Matrix	40v	"						−3.79	5.29	0.708982
M-2000	Merritton	Pentamerus oblongus	37	~ −400						−5.30	2.49	0.708291
M-2003	"	Pentamerus oblongus	37	"	1.60	5955	540	285	3.14	−6.16	2.48	
M-2007	"	Pentamerus oblongus	37	"	2.10	12,330	870	300	2.63	−5.55	2.33	
M-2007d	Merritton	Pentamerus oblongus	37	~ −400						−5.97	2.33	
M-2009	"	Pentamerus oblongus	37	"						−5.55	2.33	
M-2009d	"	Pentamerus oblongus	37	"						−5.97	2.33	
M-2010	"	Pentamerus oblongus	37	"	1.40	2260	265	130	7.08	−5.27	2.45	0.708346
M-2000m	"	Matrix	37	"						−5.82	1.99	0.708475
M-2006	"	Pentamerus oblongus	37	"	0.80	12,300	895	300	2.60			
M-2013	"	Pentamerus oblongus	37	"	0.90	2025	830	380	1.89			
Ra-2600	Reynales	Pentamerus oblongus	45	~ −675	5.00	1520	380	180	5.47	−5.12	0.46	0.708131
Ra-2600d	Wallington	Pentamerus oblongus	45	"						−5.57	1.22	
Ra-2601	"	Pentamerus oblongus	45	"	6.10	2980	2980	1065	0.65	−7.58	−0.60	
Ra-2602	"	Pentamerus oblongus	45	"	10.10	3900	1235	370	2.67			
Ra-2603	"	Pentamerus oblongus	45	"	7.90	3450	3200	1340	0.39			
Ra-2605	"	Pentamerus oblongus	45	"	5.10	1840	2935	920	0.77			
Ra-2609B	"	Pentamerus oblongus	45	"						−5.98	1.64	
Ra-2609A	"	Pentamerus oblongus	45	"						−6.11	1.68	
Ra-2610m	"	Matrix	45	"						−7.63	0.65	0.709396
N-4000	Neagha	Brach fragment	37	~ −750						−6.91	0.01	0.708228
N-4000s	"	Spar cement	37	"						−6.59	−0.71	
N-4002	"	Brach fragment	37	"						−7.04	−2.58	
N-4003	"	Brach fragment	37	"						−7.14	−2.17	
N-4004	"	Brach fragment	37	"						−7.14	−0.29	
N-4005m	"	Matrix	37	"						−8.19	0.38	

References

Auclair, A.C., Joachimski, M.M., Lecuyer, C., 2003. Decipering kinetic, metabolic and environmental controls on stable isotope fractionations between seawater and the shell of Terebratalia transversa (Brachiopoda). Chem. Geol. 202, 59–78.

Azmy, K., Veizer, J., Bassett, M.G., Copper, P., 1998. Oxygen and carbon isotopic composition of Silurian brachiopods: implications for coeval seawater and glaciations. Geol. Soc. Amer. Bull. 110, 1499–1512.

Azmy, K., Veizer, J., Wenzel, B., Bassett, M.G., Copper, P., 1999. Silurian strontium isotope stratigraphy. Geol. Soc. Amer. Bull. 111, 475–483.

Bates, N.R., 1990. Biogeochemistry of Paleozoic brachiopods from New York State and Ontario. Unpub. M.Sc. thesis, Brock University, 257 pp.

Bathurst, R.G.C., 1975. Carbonate Sediments and Their Diagenesis. Elsevier. 658 pp.

Berry, W.B.N, Boucot, A.J., 1970. Correlation of North American Silurian rocks. Geol. Soc. Amer. Spec. Pap. 102.

Bertram, C.J., Elderfield, H., Aldridge, R.J., Morris, S.C., 1992. $^{87}Sr/^{86}Sr$, $^{143}Nd/^{144}Nd$, and REEs in Silurian phosphatic fossils. Earth Planet Sci Lett. 113, 239–249.

Boucot, A.J., 1962. Appalachian Siluro-Devonian. In: Coe, K. (Ed.), Some Aspects of the Variscan Fold Belt. Manchester Univ. Press, pp. 155–163.

Brand, U., 1991. Strontium isotope diagenesis of biogenic aragonite and low-Mg calcite. Geochim. Cosmochim. Acta 55, 505–513.

Brand, U., 2004. Carbon, oxygen and strontium isotopes in Paleozoic carbonate components: an evaluation of original seawater-chemistry proxies. Chem. Geol. 204, 23–44.

Brand, U., Veizer, J., 1980. Chemical diagenesis of a multicomponent carbonate system. 1. Trace elements. J. Sediment. Petrol. 50, 1219–1236.

Brand, U., Veizer, J., 1981. Chemical diagenesis of a multicomponent carbonate system. 2. Stable isotopes. J. Sediment. Petrol. 51, 987–997.

Brand, U., Logan, A., Hiller, N., Richardson, J., 2003. Geochemistry of modern brachiopods: applications and implications for oceanography and paleoceanography. Chem. Geol. 198, 305–334.

Brand, U., Legrand-Blain, M., Streel, M., 2004. Biochemostratigraphy of the Devonian–Carboniferous boundary global stratotype section and point, Griotte Formation, La Serre, Montagne Noire, France. Palaeogeogr. Palaeoclimatol. Palaeoecol. 205, 337–357.

Brenchley, P.J., Marshall, J.D., Carden, G.A., Robertson, D.B.R., Long, D.F.G., Meidla, T., Hints, L., Anderson, T.F., 1994. Bathymetric and isotopic evidence for a short-lived Late Ordovician glaciation in a greenhouse period. Geology 22, 295–298.

Brenchley, P.J., Carden, G.A., Hints, L., Kaljo, D., Marshall, J.D., Martma, T., Meidla, T., Nolvak, J., 2003. High-resolution stable isotope stratigraphy of Upper Ordovician sequences: constraints on the timing of bioevents and environmental changes associated with mass extinction and glaciation. Geol. Soc. Amer. Bull. 115, 89–104.

Brett, C.E., Goodman, W.M., 1996. Sequence stratigraphy of central New York and central Pennsylvania: a regional synthesis. In: Broadhead, T. W. (Ed.), Sedimentary Environments of Silurian Taconia: Fieldtrips to

the Appalachians and Southern Craton of Eastern North America. Univ. Tenn. Studies in Geol., vol. 26, pp. 170–200.

Brett, C.E., Goodman, W.M., Loduca, S.T., Lehmann, D.F., 1990. Sequences, cycles, and basin dynamics in the Silurian of the Appalachian Foreland Basin. Sediment. Geol. 69, 191–244.

Brett, C.E., Tepper, D.H., Goodman, W.M., Loduca, S.T., Lin, B.-Y., 1995. Revised stratigraphy and correlations of the Niagara Provincial Series (Medina, Clinton and Lockport Groups) in the type area of western New York. U.S. Geol. Surv. Bull. 2086. 66 pp. Brett, C.E., Baarli, B.G., Chowns, T., Cotter, E., Driese, S., Goodman, W., Johnson, M.E., 1998. Early Silurian condensed intervals, ironstones, and sequence stratigraphy in the Appalachian foreland basin. In: Landing, E., Johnson, M.E. (Eds.), Silurian cycles: linkages of dynamic stratigraphy with atmospheric, oceanic, and tectonic changes. New York State Museum Bull., vol. 491, pp. 89–143.

Calner, M., Jeppsson, L., Munnecke, A., 2004. The Silurian of Gotland. Part 1. Review of the stratigraphic framework, event stratigraphy, and stable carbon and oxygen isotope development. Erlanger Geogr. Abh. 5, 113–131.

Caputo, M.V., 1996. Silurian glacial paleogeography in South America. The James Hall Symposium: Second International Symposium on the Silurian System. Univ Rochester, N.Y. 40 pp.

Caputo, M.V., 1998. Ordovician–Silurian glaciations and global sea-level changes. In: Landing, E., Johnson, M.E. (Eds.), Silurian Cycles: Linkages of Dynamic Stratigraphy with Atmospheric, Oceanic, and Tectonic Changes. New York State Museum Bull., vol. 491, pp. 15–25.

Carpenter, S.C., Lohmann, K.C., 1995. $\delta^{18}O$ and $\delta^{13}C$ values of modern brachiopod shells. Geochim. Cosmochim. Acta 59, 3749–3764.

Cummins, D.J., Elderfield, H., 1994. The strontium isotopic composition of Brigantian (Late Dinantian) seawater. Chem. Geol. 118, 225–270.

Denison, R.E., Koepnick, R.B., Burke, W.H., Hetherington, E.A., Fletcher, A., 1997. Construction of the Silurian and Devonian seawater $^{87}Sr/^{86}Sr$ curve. Chem. Geol. 140, 109–121.

Diener, A., Ebneth, S., Veizer, J., Buhl, D., 1996. Strontium isotope stratigraphy of the Middle Devonian: brachiopods and conodonts. Geochim. Cosmochim. Acta 60, 639–652.

Driese, S.G., Fischer, M.W., Easthouse, K.A., Marks, G.T., Gogola, A.R., Schoner, A.E., 1991. Models for genesis of shelf sandstone sequences, southern Appalachians: paleoenvironmental reconstruction of an Early Silurian shelf system. In: Swift, D.J.P., Oertel, G.F., Tillman, T.W., Thorne, J.A. (Eds.), Shelf Sand and Sandstone Bodies: Geometry, Facies, and Sequence Stratigraphy. Int'l. Assoc. Sed. Spec. Publ., vol. 14, pp. 309–338.

Elderfield, H., 1986. Strontium isotope stratigraphy. Palaeogeogr. Palaeoclimatol. Palaeoecol. 57, 71–90.

Ettensohn, F.R., Brett, C.E., 1998. Tectonic components in third-order Silurian cycles: examples from the Appalachian Basin and global implications. In: Landing, E., Johnson, M.E. (Eds.), Silurian Cycles: Linkages of Dynamic Stratigraphy with Atmospheric, Oceanic, and Tectonic Changes. New York State Museum Bull., vol. 491, pp. 145–162.

Grahn, Y., Caputo, M.V., 1992. Early Silurian glaciations in Brazil. Palaeogeogr. Palaeoclimatol. Palaeoecol. 99, 9–15.

Grahn, Y., Paris, F., 1992. Age and correlation of the Trombetas Group, Amazonas Basin. Brazil. Rev. Micropaleontol. 35, 20–32.

Grossman, E.L., 1992. Isotope studies of Paleozoic paleoceanography — opportunities and pitfalls. Palaios 7, 1–3.

Grossman, E.L., 1994. The carbon and oxygen isotope record during the evolution of Pangea: Carboniferous to Triassic. Geol. Soc. Amer. Spec. Pap. 288, 207–228.

Hambry, M.J., 1985. The Late Ordovician–Early Silurian glacial period. Palaeogeogr. Palaeoclimatol. Palaeoecol. 51, 273–289.

Harland, W.B., Cox, A.V., Llewellyn, P.G., Pickton, C.A.G., Smith, A.G., Walters, R., 1982. A Geologic Time Scale. Cambridge Univ. Press, Cambridge, U.K. 131 pp.

Heath, R.J., Brenchley, P.J., Marshall, J.D., 1998. Early Silurian carbon and oxygen stable-isotope stratigraphy of Estonia: implications for climate change. In: Landing, E., Johnson, M.E. (Eds.), Silurian Cycles: Linkages of Dynamic Stratigraphy with Atmospheric, Oceanic, and Tectonic Changes. New York State Museum Bull., vol. 491, pp. 313–327.

Holmden, C., Creaser, R.A., Muehlenbachs, K., Bergstrom, S.M., Leslie, S.A., 1996. Isotopic and elemental systematics of Sr and Nd in Ordovician biogenic apatites: implications for paleoseawater studies. Earth Planet. Sci. Lett. 142, 425–437.

Jeppsson, L., 1987. Lithological and conodont distributional evidence for episodes of anomalous oceanic conditions during the Silurian. In: Aldridge, R.J. (Ed.), Palaeobiology of Conodonts, vol. 1987. Ellis Horwood Ltd, Chichester, pp. 129–145.

Jeppsson, L., 1990. An oceanic model for lithological and faunal changes tested on the Silurian record. J. Geol. Soc. (Lond.) 147, 663–674.

Jeppsson, L., 1998. Silurian oceanic events: summary of general characteristics. In: Landing, E., Johnson, M.E. (Eds.), Silurian Cycles: Linkages of Dynamic Stratigraphy with Atmospheric, Oceanic, and Tectonic Changes. New York State Museum Bull., vol. 491, pp. 239–257.

Jeppsson, L., Aldridge, R.J., Dorning, K.J., 1995. Wenlock (Silurian) oceanic episodes and events. J. Geol. Soc. (Lond.) 152, 487–498.

Johnson, M.E., 1996. Stable cratonic sequences and a standard for Silurian eustasy. In: Witzke, B.J., Ludvigson, G.A., Day, J.E. (Eds.), Paleozoic Sequence Stratigraphy: Views From the North American Craton. Geol. Soc. Am., Spec. Paper, vol. 306, pp. 203–211.

Johnson, M.E., Rong, J.Y., Kershaw, S., 1998. Calibrating Silurian eustasy against the erosion and burial of coastal paleotopography. In: Landing, E., Johnson, M.E. (Eds.), Silurian Cycles: Linkages of dynamic Stratigraphy with Atmospheric, Oceanic, and Tectonic Changes. New York State Museum Bull., vol. 491, pp. 3–13.

Kidwell, S.M., Bosence, D.W.J., 1991. Taphonomy and time-averaging of marine shelly faunas. In: Allison, P.A., Briggs, D.E.G. (Eds.), Taphonomy: Releasing the Data Locked in the Fossil Record. Plenum Press, pp. 116–209.

Kleffner, M.A., 1989. A conodont-based Silurian chronostratigraphy. Geol. Soc. Amer. Bull. 101, 904–912.

Kleffner, M.A., 1991. Conodont biostratigraphy of the upper part of the Clinton Group and the Lockport Group (Silurian) in the Niagara Gorge Region, New York and Ontario. J. Paleontol. 65, 500–511.

Lécuyer, C., Allemand, P., 1999. Modeling of the oxygen isotope evolution of seawater: implications for the climate interpretation of the $\delta^{18}O$ of marine sediments. Geochim. Cosmochim. Acta 63, 351–361. Lee, X., Hu, R., Brand, U., Zhou, H., Liu, X., Yuan, H., Yan, C., Cheng, H., 2004. Ontogenetic trace element distribution in brachiopod shells: an indicator of original seawater chemistry. Chem. Geol. 209, 49–65.

Loduca, S.T., Brett, C.E., 1994. Revised stratigraphic and facies relationships of the lower part of the Clinton Group (Middle Llandoverian) of western New York State. In: Landing, E. (Ed.), Sea-level Changes, an Integrated Approach. Soc. Econ. Paleon. Min. Spec. Publ., vol. 42, pp. 183–213.

Marshall, J.D., Brenchley, P.J., Mason, P., Wolff, G.A., Astini, R.A., Hints, L., Meidla, T., 1997. Global carbon isotopic events associated with mass extinction and glaciation in the Late Ordovician. Palaeogeogr. Palaeoclimatol. Palaeoecol. 132, 195–210.

Meyers, K.J., Milton, N.J., 1996. Concepts and principles of sequence stratigraphy. In: Emery, D., Meyers, K.J. (Eds.), Sequence Stratigraphy. Blackwell Sci. Ltd, Oxford, pp. 11–44.

Melchin, M.J., 1994. Graptolite extinction at the Llandovery–Wenlock boundary. Lethaia 27, 285–290.

Melchin, M.J., Koren, T.N., Storch, P., 1998. Gobal diversity and survivorship patterns of Silurian graptoloids. In: Landing, E., Johnson, M.E. (Eds.), Silurian Cycles: Linkages of Dynamic Stratigraphy with Atmospheric, Oceanic, and Tectonic Changes. New York State Museum Bull., vol. 491, pp. 165–182.

Mii, H.-S., Grossman, E.L., Yancey, T.E., 1999. Carboniferous isotope stratigraphies of North America: implications for Carboniferous paleoceanography and Mississippian glaciation. Geol. Soc. Amer. Bull. 111, 960–973.

Muehlenbachs, K., 1998. The oxygen isotopic composition of the oceans, sediments and the seafloor. Chem. Geol. 145, 263–273.

Munnecke, A., Samtleben, Ch., Bickert, T., 2003. The Ireviken event in the Lower Silurian of Gotland, Sweden — relation to similar Palaeozoic and Proterozoic events. Palaeogeogr. Palaeoclimatol. Palaeoecol. 195, 99–124.

Parkinson, D., Curry, G.B., Cusack, M., Fallick, A.E., 2005. Shell structure, patterns and trends of oxygen and carbon stable isotopes in modern brachiopod shells. Chem. Geol. 219, 193–235.

Popp, B.N., Anderson, T.F., Sandberg, P.A., 1986. Brachiopods as indicators of original isotopic compositions in some Paleozoic limestones. Geol. Soc. Amer. Bull. 97, 1262–1269.

Qing, H., Barnes, C.R., Buhl, D., Veizer, J., 1998. The strontium isotopic composition of Ordovician and Silurian brachiopods and conodonts: relationships to geological events and implications for coeval seawater. Geochim. Cosmochim. Acta 62, 1721–1733.

Rexroad, C.B., Richard, L.V., 1965. Zonal conodonts from the Silurian of the Niagara Gorge. J. Paleontol. 39, 1217–1220.

Ruppel, S.C., James, E.W., Barrick, J.E., Nowlan, G., Uyeno, T.T., 1996. High-resolution $^{87}Sr/^{86}Sr$ chemostratigraphy of the Silurian: implications for event correlation and strontium flux. Geology 24, 831–834.

Ruppel, S.C., James, E.W., Barrick, J.E., Nowlan, G., Uyeno, T.T., 1998. High-resolution Silurian $^{87}Sr/^{86}Sr$ record: evidence of eustatic control of seawater chemistry? In: Landing, E., Johnson, M.E. (Eds.), Silurian Cycles: Linkages of Dynamic Stratigraphy with Atmospheric, Oceanic, and Tectonic Changes. New York State Museum Bull., vol. 491, pp. 285–295.

Saltzman, M.R., 2001. Silurian $\delta^{13}C$ stratigraphy: a view from North America. Geology 29, 671–674.

Saltzman, M.R., Runnegar, B., Lohmann, K.C., 1998. Carbon isotope stratigraphy of Upper Cambrian (Steptoean Stage) sequences of the eastern Great Basin: record of a global oceanographic event. Geol. Soc. Amer. Bull. 110, 285–297.

Samtleben, C., Munnecke, A., Bickert, T., Pätzold, J., 1996. The Silurian of Gotland (Sweden): facies interpretation based on stable isotopes in brachiopod shells. Geol. Rundsch. 85, 278–292.

Samtleben, C., Munnecke, A., Bickert, T., Pätzold, J., 2001. Shell succession, assemblage and species dependent effects on the C/O-isotopic composition of brachiopods — examples from the Silurian of Gotland. Chem. Geol. 175, 61–107.

Scotese, C.R., Golonka, J., 1992. PALEOMAP Paleogeographic Atlas. PALEOMAP Progress Report #20. Univ. Texas.

Spooner, E.T.C., 1976. The strontium isotopic composition of seawater and seawater–oceanic crust interactions. Earth Planet. Sci. Lett. 31, 167–174.

Storch, P., 1995. Biotic crises and post-crisis recoveries recorded by graptolite faunas of the Barrandian area (Czech Republic). Geolines 3, 59–70.

Talent, J.A., Mawson, R., Andrew, A.S., Hamilton, P.J., Whitford, D.J., 1993. Middle Palaeozoic extinction events: faunal and isotopic data. Palaeogeogr. Palaeoclimatol. Palaeoecol. 104, 139–152.

Tucker, R.D., McKerrow, W.S., 1995. Early Paleozoic chronology: a review in light of new U–Pb zircon ages from Newfoundland and Britain. Can. J. Earth Sci. 32, 368–379.

Vail, P.R., Mitchum Jr., R.M., Thompson III, S., 1977. Seismic stratigraphy and global changes in sea level. Part 4. Global cycles of relative changes in sea level. In: Peyton, C.E. (Ed.), Seismic Stratigraphy — Applications to Hydrocarbon Exploration. Amer. Assoc. Petrol. Geol., vol. 26, pp. 83–97.

Veizer, J., 1989. Strontium isotopes in seawater through time. Ann. Reviews Earth Planet. Sci. 17, 141–167.

Veizer, J., Buhl, D., Diener, A., Ebneth, S., Podlaha, O.G., Bruckschen, P., Jasper, T., Korte, C., Schaaf, M., Ala, D., Azmy, K., 1997. Strontium isotope stratigraphy: potential resolution and event correlation. Palaeogeogr. Palaeoclimatol. Palaeoecol. 132, 65–77.

Veizer, J., Ala, D., Azmy, K., Bruckschen, P., Buhl, D., Bruhn, F., Carden, G.A.F., Diener, A., Ebneth, S., Goddéris, Y., Jasper, T., Korte, C., Pawellek, F., Podlaha, O.G., Strauss, H., 1999. $^{87}Sr/^{86}Sr$, $\delta^{13}C$ and $\delta^{18}O$ evolution of Phanerozoic seawater. Chem. Geol. 161, 59–88.

Wadleigh, M.A., Veizer, J., 1992. $^{18}O/^{16}O$ and $^{13}C/^{12}C$ in Lower Paleozoic articulate brachiopods: implications for the isotopic composition of seawater. Geochim. Cosmochim. Acta 56, 431–443.

Walliser, O.H., 1964. Conodonten des Silurs. Abh. Hess. Landesamtes Bodenforsch., Wiesbaden 41.

Wallmann, K., 2001. The geological water cycle and the evolution of marine $\delta^{18}O$ values. Geochim. Cosmochim. Acta 65, 2469–2485.

Wenzel, B., Joachimski, M.M., 1996. Carbon and oxygen isotopic composition of Silurian brachiopods (Gotland/Sweden): palaeoceanographic implications. Palaeogeogr. Palaeoclimatol. Palaeoecol. 122, 143–166.

Wilde, P., 1991. Oceanography in the Ordovician. In: Advances in Ordovician geology. In: Barnes, C.R., Williams, S.H. (Eds.), Geol. Surv. Can. Paper, vol. 90-9, pp. 283–298.

Wilde, P., Berry, W.B.N., Quinby-Hunt, M.S., 1991. Silurian oceanic and atmospheric circulation and chemistry. In: Bassett, M.G., Lane, P.D., Edwards, D. (Eds.), The Murchison Symposium. Spec. Papers Paleon., vol. 44, pp. 123–143.